SAPIENZA
UNIVERSITÀ DI ROMA

DIPARTIMENTO DI MEDICINA SPERIMENTALE

DOTTORATO DI RICERCA IN "PATOLOGIA UMANA"

XXV CICLO: 2009 - 2012

The role of SIRT3 in mitochondrial homeostasis and in cell survival

Candidata: Pellegrini Laura

Coordinatore: Prof. Russo Matteo Antonio

Relatore: Dr. Tafani Marco

INDEX

1. INTRODUCTION

1.1 Discovery of the sirtuins

The silent information regulator (Sir2) is the founding member of a large family of nicotinamide (NAM) adenine dinucleotide $(NAD)^+$-dependent protein deacetylases called Sirtuins, phylogenetically conserved in eukaryotes, prokaryotes, and Archeal species. To date, one or more Sirtuins have been identified in nearly every species examined.

It is a little known fact that the first sirtuin gene, *SIR2* from *Saccharomyces cerevisiae*, was originally known as *MAR1* (for mating-type regulator 1). Klar and colleagues [1] discovered *MAR1* by virtue of a spontaneous mutation that caused sterility by relieving silencing at the mating-type loci *HMR* and *HML* on chromosome III. A variety of additional mutations with a sterile phenotype were subsequently co-discovered by Jasper Rine, who named the set of four genes responsible silent information regulator (SIR)1–4 [2], thereby replacing the MAR nomenclature. Ten years after these initial finding, Gottlieb and Esposito [3] demonstrated that SIR2 was the only SIR gene required to suppress recombination between the tandemly repeated ribosomal RNA genes on chromosome XII [3]. Gottschling and colleagues in 1991, reported that SIR2 was involved in the mechanism of transcriptional repression near telomeres [4]. This transcriptional silencing at telomeres and the HM loci was showed to be associated with a relatively histones hypoacetylation at the e-amino group of N-terminal lysine residues and the overexpression of SIR2 was demonstrate to cause substantial histone deacetylation, an additional characteristic that distinguished SIR2 from the other SIR genes [5].

In the following years were identified four additional S. cerevisiae genes with high homology to SIR2 called HST for homologues of SIR2, 1-4 [6,7]. None of the four genes were essential, but they all were involved in silencing at the mating-type loci and telomeres, as well as cell-cycle progression and genomic integrity. Shortly thereafter SIR2 homologues were discovered in yeast and in other organism ranging from bacteria to mammals demonstrated that SIR2 was only one member of a large family of broadly conserved proteins we now refer to as sirtuins.

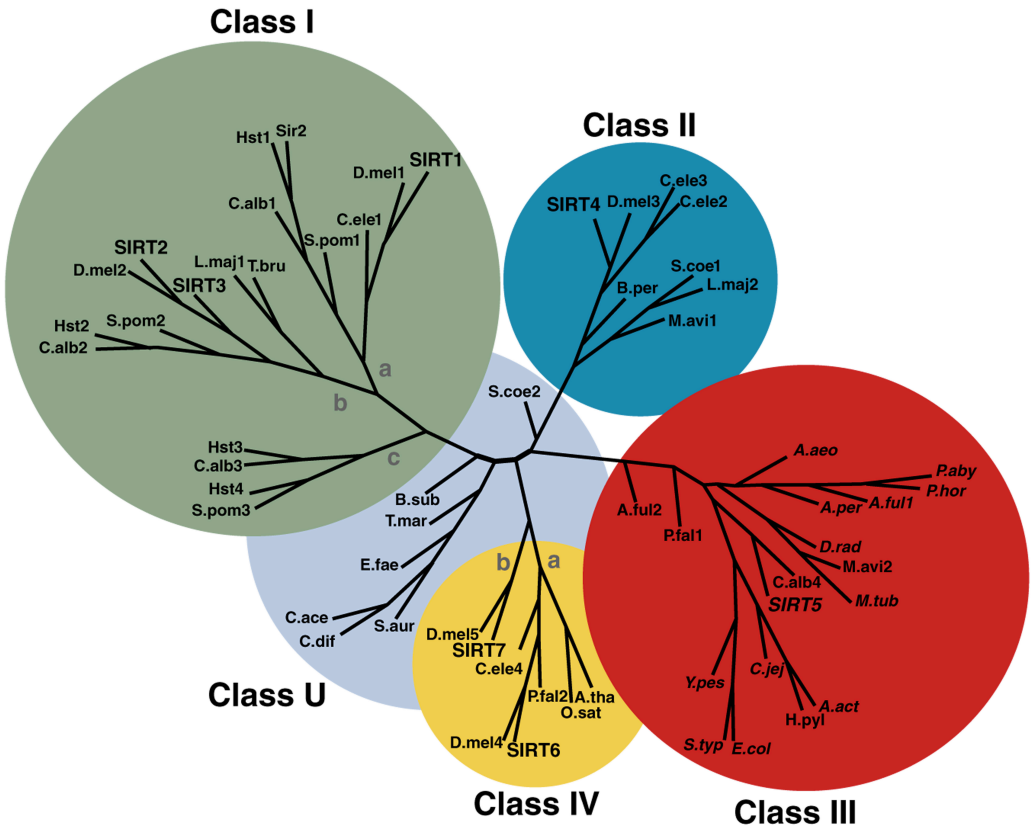

Figure 1. An unrooted tree diagram of a phylogenetic analysis of the conserved sirtuin core deacylase domain sequences, divided into class I, II, III, IV, and U groups [8]

1.2 Phylogenetic distribution of sirtuins

Based on phylogenetic tree analysis of amino acid sequence, Sirtuins have been organized into five different classes designated I, II, III, IV, and U [9] (Figure 1). The five sirtuin genes of the completely sequenced *S. cerevisiae* are all of class I subtypes; thus this yeast has evolved to survive in the absence of non-class I sirtuins. However, except for yeasts most eukaryotic organisms seem to harbor an assortment of both non-class I and class I sirtuin genes. Many types of eukaryotes have class II and class IV sirtuins. The class III sirtuin is the most widely distributed form found in prokaryotes, thus it may be a very ancient version of the sirtuin gene. Protozoans and metazoans from diverse phyla have class I and class IV sirtuins, so these types of sirtuins must have developed at an early stage of eukaryotic evolution. Thus this model postulates that an early eukaryote possessed all four types of sirtuins and that later some eukaryotes lost one (e.g., *Drosophila* and *C. elegans* which lack class III) or more (e.g., *S. cerevisiae* which lacks classes II, III, and IV) of the non-class I sirtuins [10].

1.3 Structure

A number of sirtuins from different organisms have been crystallized [11-16]. All Sirtuins share a conserved catalytic core of ~275 amino acids that is flanked by N- and C-terminal extensions. The extensions are variable in length and sequence, and they have been reported to play various roles such as ensuring a proper cellular localization, regulating the oligomerization state, and/or exerting autoregulation mechanisms [15,17,18].

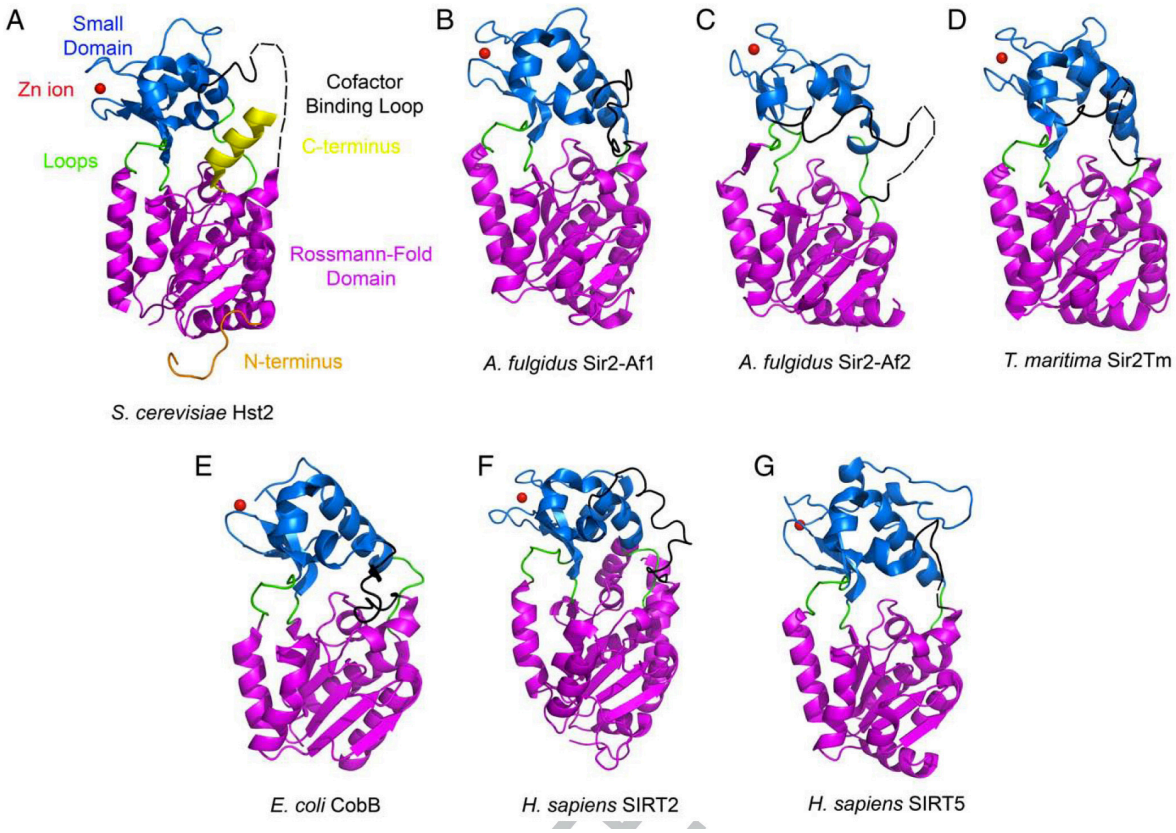

Figure 2. Three-dimensional structure of some sirtuin protein that has been determined. The enzymes are shown in cartoon representation without bound ligands. The Rossmann-fold domain is indicated in magenta, the small domain in blue, the loops in green, the cofactor binding loop in black, the Zn ion in red, the N-terminal region in orange, and the C-terminal region in yellow. Disordered regions are indicated with dashed lines [19].

The catalytic core adopts an oval-shaped fold composed of two globular subdomains linked by four loops, which contribute to the active site cleft between the subdomains [19]. This structure allows the majority of sirtuins to function as NAD^+-dependent protein deacetylases. However the same domain in some sirtuins acts as ADP- ribosyltransferase and this specialized type of sirtuins appears currently restricted to class II. The larger domain has a classical open α/β Rossmann-fold structure, which is commonly found in proteins that bind NAD^+/NAD or $NADP^+$/NADPH [20]. Six parallel β strands form a central

β sheet that is sandwiched between several α helices (the exact number of α helices depends upon the specific sirtuin protein) on either side of the β sheet [10]. The small domain shows the highest diversity among family members in term of primary sequence, three-dimensional structure and position relative to the large domain [19] and results from two insertions within the Rossmann fold domain; one comprises a zinc-binding module that contains a structural zinc atom coordinated by four invariant cysteines and the other forms a helical module that includes a flexible loop. The relative orientations of the small and the Rossmann-fold domain appear to be influenced by ligand binding as well as contact with other proteins. Both the acetylated lysine-containing polypeptide substrates and the NAD^+ co-substrate bind to the cleft at the interface of the two domains. The so-called "cofactor binding loop" shows high flexibility and its conformation was shown to evolve in close relation to the catalytic events [19].

1.4 Enzymatic activity

The most prominent enzymatic activity of sirtuins is represented by the NAD^+-dependent e–*N*-acetyl-lysine deacetylation of histones and non-histone proteins [21-25]. The deacetylation reaction consumes NAD^+ as a substrate and results in the production of deacetylated substrate, nicotinamide and 2'-*O*-acetyl-ADP-ribose (2'-AADPR) [26,27]. The proposed mechanism of sirtuin catalysis is called the ADPR-peptidyl-imidate mechanism and is a six-step reaction [28] (Figure 3).

Briefly, the deacetylation reaction begins with an amide cleavage of NAD^+ and the formation of nicotinamide (NAM) and a covalent ADP ribose (ADPR) peptide-imidate intermediate. The intermediate is resolved to form AADPR, and the deacetylated substrate is released [27,29,30]. Although the amide-to-AADPR acyltransfer is unfavorable, hydrolysis of NAD^+ can provide a favorable driving force for the overall sirtuin reaction [28,31,32]. Even if some details of the catalytic reaction remain to be resolved, it is thought that peptide binding facilitates an allosteric change in enzyme structure that enables reaction of NAD+ with a nucleophile from the enzyme to generate the enzyme-stabilized ADPR intermediate [28].

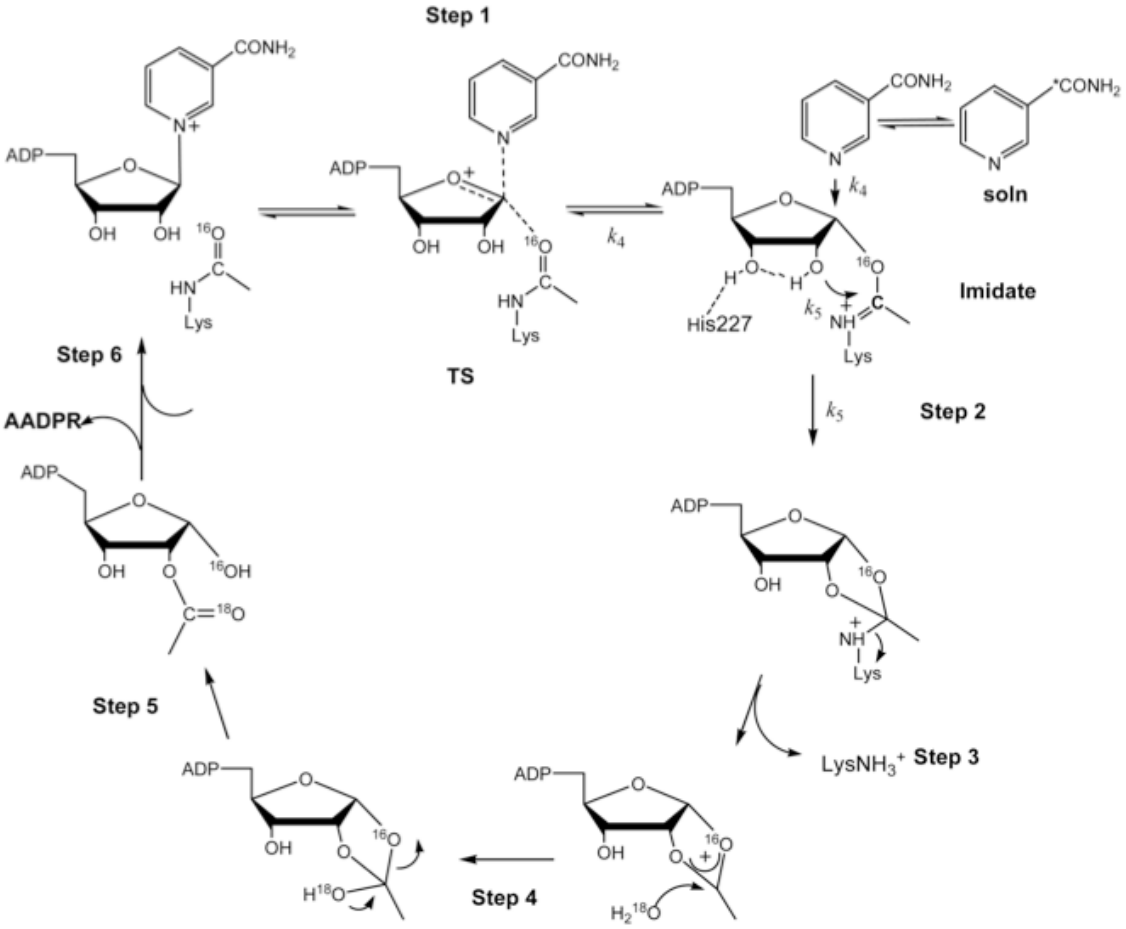

Figure 3. Proposed reaction mechanism of sirtuin catalyzed NAD+-dependent deacetylation [33].

In several reports, sirtuins were suggested to harbour also a NAD^+-dependent ADP-ribosyltransferase activity, transferring ADP-ribose to a protein acceptor or to the enzyme itself [10,25,34-36]. Based on the established NAD^+-dependent deacetylation reaction mechanism, several ADP- ribosylation mechanisms have been proposed. One mechanism is similar to the first step of the deacetylation mechanism, which involves the attack of the 1′ position of NAD by a nucleophilic residue from substrate proteins [37-39].

The second mechanism suggests that the alkylimidate intermediate formed in the deacetylation reaction could be captured by nucleophilic residues of protein, resulting in protein ADP-ribosylation [38,39]. Both mechanism are the direct consequence of sirtuin's catalytic action, and thus are called "enzymatic ADP-ribosylation. In contrast, also other two mechanisms have been proposed that are indirect consequence of the enzymatic action of sirtuins. One mechanism suggests that the 2'-O-acetyl ADP-ribose generated in the deacetylation reaction non-specifically reacts with the nucheophilic residues such as Lys

and Cys. Similarly, in the absence of deacetylation substrates, sirtuins could generate ADP ribose, which could also react with proteins non-enzymatically [39].

Other enzymatic activities that has been described for the sirtuins are desuniccinylation, demalonylation, depropionylation and debutyrylation [39-42]. It has therefore been suggested that sirtuins should be redefined as ‘‘deacylases’’ rather than deacetylases [39].

These activities are directly controlled by cellular NAD+ levels, which is an indicator of cellular metabolic status and are inhibited by nicotinamide, the enzymatic product of the deacetylaytion reaction [43], and possibly by NADH [44].

1.5 Mammalian Sirtuin

In mammalian seven sirtuin, SIRT1-7, have been identified and based on the phylogenetic analysis they have been divided into four classes: SIRT1– SIRT3 belong to class I, SIRT4 to class II, SIRT5 to class III, and SIRT6 and SIRT7 to class IV [9]. Although these sirtuins are relatively conserved, their N and C termini differ, and they are likely to have highly divergent biological functions owing to (a) different enzymatic activities, (b) distinct subcellular localization and expression pattern and (c) unique binding partners and substrates.

Deacetylation is the most prominent activity of SIRT1 [25] and SIRT2 [45]. In contrast, SIRT4 [36] and SIRT6 [46] possess mostly mono-ADP-ribosyl transferase activity. SIRT3 [47] and SIRT1 [36,46,48] possess both activities. SIRT5 was originally reported to deacetylate CPS1 [49], but its demalonylation [39,40] and desuccinylation [39] actions on CPS1 and other proteins now seem more important.

SIRT1 is the closest human homologue to the founding yeast Sir2 [10]. It is mainly localized in the nucleus, but it shuttles to the cytoplasm when required to act on cytoplasmic targets [50] such as during inhibition of insulin signaling [51]. SIRT1 interacts with and regulates a number of histone and non-histone protein substrates. It is involved in energy metabolism, inflammation and in the repair of DNA double-strand break, among others.

SIRT2 localizes primarily in the cytoplasm. It deacetylates tubulin microtubules [52] and transcription factors that shuttle from the cytoplasm to the nucleus [53]. Moreover it plays an important role in cell cycle regulation; during mitosis SIRT2 is required for exit of cells from the mitotic phase [54]. It localizes to chromatin and deacetylates acetylated histone H4K16, and thus decreases the latter during G2/M transition [55]. SIRT2 is thereby pivotal to formation of condensed chromatin when the latter must be generated anew [55]. Moreover by deacetylating BubR1 kinase, it may help ensure faithful chromosome separation during

mitosis [56]. This protein is also involved in the regulation of the metabolism through the deacetylation and stabilization of phosphoenolpyruvate carboxykinase (PEPCK1), which is the rate limiting enzyme for gluconeogenesis, linking SIRT2 with type II diabetes [57]. SIRT2 mediates also the response to nutrient deprivation and energy expenditure by promoting lipolysis and inhibiting adipocyte differentiation through deacetylation of Forkhead box O (FoxO) [53]. Other deacetylation targets of SIRT2 in the cytoplasm are p65, a subunit of NF-κB, [58] and the acetyl-transferase p300 [59]. Furthermore a recent work suggested a role for SIRT2 in regulating necroptosis through the deacetylation of RIP1 [60].

SIRT6 is a nuclear, chromatin-bound protein [61] and plays an essential role in animal development. SIRT6 null mice appear to have normal embryonic development and intrauterine growth and born without obvious abnormalities. However, they suffer a severe metabolic imbalance, acute onset of hypoglycemia, postnatal growth retardation, and premature death at one month of age [61]. SIRT6 is a highly specific histone 3 deacetylase that targets acetyl-H3K9 and acetyl-H3K56, playing an important role in DNA repair, telomere function, genomic stability, and cellular senescence [50,62-65]. Moreover SIRT6 appears to have particular significance in regulating metabolism. Indeed, it co-represses hypoxia-inducible factor 1α (HIF1α) to suppress glucose uptake and glycolysis [46]. SIRT6 also plays a key role in transcriptional regulation via NF-κB [66] and seems the only sirtuin linked to the regulation of immune responses [67].

SIRT7 resides mainly in the nucleolus where it is associated with active ribosomal RNA genes and binds to histone and RNA polymerase I to stimulate transcription [68]. The biochemical activity, molecular targets and physiological functions of this sirtuin have been unclear. It has been demonstrate to be relevant for the reactivation of rDNA transcription at the end of mitosis [69] and has been proposed to have a role as a principal activator of proliferation [50]. Moreover it seems to be crucial for maintenance of oncogenic transformation [70]. Mice with SIRT7 deletion develop inflammatory cardiomyopathy, cardiac hypertrophy, fibrosis, increased collagen III accumulation, hyperacetylation of p53, increased apoptosis, and reduced resistance to oxidative stress [71].

1.6 Mitochondrial sirtuins

In mammalian there are three sirtuins SIRT3, SIRT4, and SIRT5, that localized in the mitochondria [50] and regulate several aspects of mitochondrial physiology by controlling post-translational modifications of mitochondrial protein and transcription of mitochondrial genes [72].

SIRT4 is present in the mitochondrial matrix [73] and appears to be involved primarily in metabolism. Thus far, no deacetylase function of SIRT4 has been detected, but has been demonstrate a weak ADP-ribosyltransferase activity [73-76]. By ADP-ribosylation SIRT4 regulates the activity of GDH-1 limiting the metabolism of glutamate and glutamine to generate ATP during calorie-sufficient conditions [73]. Moreover, recently has been shown that through the inhibition of GDH-1 it modulates the sensitivity to PTP induction [76].

Also SIRT5 localized in the mitochondrial matrix and it seems to be involved in the control of urea cycle. Indeed, it was reported to interact with carbamoyl phosphate synthetase I (CPS1), which catalyzes the first, rate-limiting step of the urea cycle for ammonia detoxification and disposal [49]. A recent work suggest SIRT5 as the major protein demalonylase and desuccinylase in mammals since mice lacking this sirtuin exhibit global protein hypermalonylation and hypersuccinylation [40].

1.7 SIRT3

SIRT3 was the first mammalian sirtuin shown to be localized to mitochondrial matrix [17,50,77] and is considered the major mitochondrial deacetylase based on the fact that tissues from SIRT3$^{-/-}$ mice exhibit striking mitochondrial protein hyperacetylation [78,79]. However, in the last years the exact SIRT3 localization has been the subject of controversy. Initial studies had indicated that it was localized to the mitochondrial matrix and cleavage of its signal sequence was necessary for its enzymatic activity [17], but subsequent reports have suggested that SIRT3 resides in the nucleus and exerts epigenetic control through the deacetylation of histone substrates [80,81], questioning the exclusively mitochondrial distribution. The ambiguity likely arises from the two different isoforms (short and full length) of SIRT3 which are expressed in both mice and humans [82].

Schewer et al. had suggested that hSIRT3 is synthesized as a full-length (FL), inactive precursor within the cytoplasm, transported to the mitochondrial matrix, where it is proteolytically processed to activate its enzymatic potential [17]. However subsequent studies demonstrated that the full-length SIRT3 is expressed in the nucleus as well, and that both forms exhibit deacetylase activity that requires NAD^+ [80,81,83]. Recently has been reported that the FL form undergoes rapid degradation in response of cellular stress condition, including DNA damage, resulting in the de-repression of nuclear genes that encode proteins involved in sensing metabolic stress [84].

In the mitochondria SIRT3 is responsible for the deacetylation of enzymes involved in diverse functions, including energy production, antioxidant defense and cellular resistance

towards stress conditions, indicating that SIRT3 activity may ensure coordinated regulation of several distinct mitochondrial functions [85].

SIRT3 deacetylates and diminishes the activity of cyclophilin D, thereby, promoting the dissociation of hexokinase II from the mitochondrial membrane and slowing down the entry of glucose into glycolysis. Moreover it plays an important role in the regulation of the oxidative phosphorylation (OXPHOS), the process by which mitochondria generate ATP, influencing multiple step of this process. It is reported, indeed, that SIRT3 physically associates with complexes I, II, and V; in particular, it can deacetylate NDUFA11 and NDUFS8 subunits of complex I [86,87], SDHA and SDHB of complex II [87,88], III the 56 kDa core I subunit of complex III [89] and the ATP5A1, ATP5B1 and ATP5F1 subunits of complex V [87]. All these subunits are hyperacetylated in SIRT3 KO cells.

Furthermore SIRT3 has been found to be involved in the regulation of other mitochondrial metabolic pathways, in particular it stimulates fatty acid oxidation by deacetylating long chain acyl-CoA dehydrogenase (LCAD) [90] and activates glutamate dehydrogenase (GDH) to increase amino acid oxidation via the tricarboxylic acid (TCA) cycle [91]. It has also been demonstrated that it has a role in the ketone body metabolism through the deacetylation of 3-hydroxy-3-methylglutaryl CoA synthase 2 (HMGCS2) [92] and of acetyl-CoA synthase 2 (AceCS2) [93,94]. Moreover through the deacetylation and the consequent activation of the ornithine transcarbamoylase, a key enzyme responsible for the detoxification of ammonia during amino acid metabolism, SIRT3 modulates also the urea cycle. [95].

In the mitochondria, as well as in the nucleus, SIRT3 has been demonstrated to be a key regulator of cell defense and survival in response to various forms of stress mainly maintaining mitochondrial integrity and genomic stability. Has been reported that SIRT3 could influence cell survival by regulating the state of the mitochondrial permeability transition pore (MPT). However, the precise effects of SIRT3 on MPT are still not clear. In fact, some reports have shown that SIRT3 would deacetylate and inhibit the enzymatic activity of cyclophilin D [96] with the following dissociation from adenine nucleotide translocator, which, in turn, promotes detachment of hexokinase II (HKII) from voltage-dependent anion channel. Inhibition of cyclophilin D is thought to decrease the probability of pore opening [97]. Importantly, inhibition of SIRT3 activity by treating cells with ethanol enhanced the sensitivity of mitochondria to induction of MPT by increasing cyclophilin D activity [98]. By contrast, it has also been reported that in some instances cyclophilin D prevents apoptotic cell death through modulation of Bcl-2 and by promoting the binding of HKII to the mitochondria [99,100]. Shulga et al. demonstrated that a decrease of sirtuin 3 activity enhances the binding of HKII to the mitochondria by increasing cyclophilin D

activity, potentially making the cells resistant to apoptosis [96].

Moreover a protective role of SIRT3 from apoptotic cell death following genotoxic or oxidative stress has been described in cardiomyocytes [101]. They demonstrated that SIRT3 deacetylates Ku70, a DNA-repair factor and inhibitor of Bax-mediated apoptosis, promoting its interaction with the proapoptotic protein Bax. Thus, under stress conditions, increased expression of SIRT3 protects cardiomyocytes, in part by hindering the translocation of Bax to mitochondria.

SIRT3 has been shown to regulate the production of reactive oxygen species (ROS) at the level of the electron transport chain (ETC) as well as the detoxification of ROS through activation of antioxidant enzymes [83,86,102-105]. In particular it has been demonstrated that SIRT3 deacetylates Forkhead box O3a (Foxo3a) inducing the transcription of anti-oxidant-enconding genes such as manganese superoxide dismutase (MnSOD) and catalase (Cat) [83,105] and deacetylates and activates mitochondrial isocitrate dehydrogenase 2 (IDH2), leading to increased NADPH levels and an increased ratio of reduced to oxidized glutathione in mitochondria [104]. Moreover it deacetylates two critical lysine residues on superoxide dismutase 2 (SOD2) promoting its antioxidative activity [102,103].

Due to these fundamental roles, SIRT3 loss is related to numerous age-related pathologies, such as hearing loss [104], cardiac hypertrophy [106] and tumorigenesis [107].

There is some evidence that SIRT3 acts as a mitochondrial tumor suppressor [107]. Loss of SIRT3 results in an elevation in ROS that increases stabilization of hypoxia-inducible factor alpha (HIF-α) and thereby increases expression of HIF-dependent genes, metabolic reprogramming toward glycolysis, and a drive toward tumor phenotype [108]. The role of SIRT3 in the regulation of HIF-α will be described later. However, whether SIRT3 serves as a tumor suppressor or promoter is controversial [109]. For example, SIRT3 levels are reduced in breast cancer, consistent with its tumor suppressor role [107], but in malignant, lymph node-positive, breast cancer SIRT3 is increased [110]. SIRT3 is downregulated in hepatocellular carcinoma tissue [111]. Adenovirus-mediated overexpression of SIRT3 inhibited hepatoceullar carcinoma cell growth and induced apoptosis [111]. This was associated with NAD+ suppression, reduction in ERK1/2 signaling, activation of AKT and JNK signaling, and, by downregulation of NDM2, in reduced p53 degradation and thus increased p53 levels [111]. Oral squamous cell carcinoma cells exhibiting resistance to anoikis (a form of programmed cell death) have elevated SIRT3 expression, which may have arisen from reduced RIP. Inhibition of SIRT3 inhibits anoikis resistance in this cancer and lowers tumor incidence [112]. Thus, seems that SIRT3 role must not be generalized, but should be

examined in each cancer type separately to determine whether it functions as a tumor promoter or suppressor [109].

1.8 Hypoxia

SIRT3 has been demonstrated to play an important role in the tumor through the regulation of HIF-1, the master regulator of the adaptive response to hypoxia.

The term hypoxia refers to subnormal levels of oxygen in air, blood and tissue. The presence of hypoxic regions in a solid tumor has been known since the 1950s due to pioneering work by Gray and Thomlinson [113,114]. Oxygen diffuses to a distance of 100–150 μm from blood vessels in normal and malignant tissues. At a greater distance, the oxygen tension decreases gradually until becomes close to zero and cells that do not manage to adapt to oxygen and nutrient deprivation undergo cell death by apoptosis and /or necrosis. Paradoxically, hypoxia can also affect tumor growth positively by local adaptation, which provokes a more aggressive tumor phenotype [115].

HIF-1 is a basic helix-loop-helix heterodimeric transcription factor consisting of HIF alpha and HIF beta subunits. To date, three HIFα (HIF-1α, HIF-2α, HIF-3α) subunits and one HIFβ are know. While the HIF-1β/ARNT subunit is nuclear and constitutively expressed, HIFα is cytoplasmic and regulated by oxygen level [116,117]. In the presence of oxygen, indeed, the alpha subunit is subjected to hydroxylation by prolyl-4-hydroxylase domain proteins (PHDs) at the level of conserved proline, allowing their recognition and ubiquitination by the VHL E3 ubiquitin ligase and the consequent proteasomal degradation of the protein [118]. Under hypoxic conditions, the rate of hydroxylation declines, since the PHDs utilize oxygen as a cosubstrate. Moreover the limited oxygen increases mitochondrial ROS that, in turn, inactivate PHDs, through oxidation of the ferrous ion that is essential for their catalytic mechanism, and hence stabilize HIF-1α. So, in hypoxic condition, HIF-1α translocates from the cytoplasm to the nucleus, where it dimerizes with HIF-1β, and forms the HIF complex that binds to hypoxia-response elements (HREs) in the promoters of HIF-responsive genes [119-121].

Activation of the HIF transcription factor signalling cascade leads to extensive changes in gene expression, which allow cells, tissues and organisms to adapt to reduced oxygenation. Indeed HIF is responsible for the transcription of hundreds of genes that encode protein involved in oxygen delivery, glucose metabolism and survival. Moreover, it plays a crucial role in tumorigenesis since it regulates protein involved in every aspect of cancer biology, including: cell immortalization and stem cell maintenance; genetic instability; glucose and

energy metabolism; vascularization; autocrine growth factor signaling; invasion and metastasis; immune evasion; and resistance to chemotherapy and radiation therapy [122]. It has been shown that SIRT3, by regulating ROS, directly influence HIF-1α stability and target gene expression [108,123]. Indeed, loss of SIRT3 increased cellular HIF-1α levels by inhibiting prolyl hydroylases via an increase in cellular ROS levels due to the hyperacetylation of scavenger proteins. SIRT3, therefore, opposes reprogramming of cancer cell metabolism. [108]. Tumor cells, indeed, exhibit aberrant metabolism characterized by high glycolysis even in the presence of oxygen [124]. This preferential use of aerobic glycolysis, termed the Warburg effect, has emerged as a metabolic hallmark of many cancer. The increased glucose uptake and catabolism conferrers potential survival and proliferative advantages to cancer cells; enhanced catabolism of glucose contributes to the raw materials needed to synthesize the nucleotides, amino acids, and lipids necessary for cellular proliferation [125] and constitutive upregulation of aerobic glycolysis provide a survival advantage for tumor cells under hypoxia [126].

Other sirtuins, have been demonstrated to be implicated in the regulation of HIF-1α. SIRT1 has been reported to deacetylate both HIF-1α [127] and HIF-2α [128] causing a decrease and, unexpectedly, an increase in transcriptional activity, respectively. SIRT1, in turn, was shown to be upregulated by both HIF-1α and HIF-2α under hypoxia, which suggests that SIRT1 may play a role in negative- and positive-feedback loops that govern HIFα activity [129]. In contrast, SIRT6 may negatively regulate HIF-1α stability and protein synthesis via a yet to be defined mechanism, and may also serve, as previous described, as a HIF-1α corepressor to impede the induction of HIF1α-responsive genes.

1.9 Cell death

Under stress conditions cells can undergo to cell death. Based on morphological and biochemical features is it possible to classify different cell death subroutines. Recently the Nomenclature Committee on Cell Death (NCCD) has proposed a revised functional classification of the different type of cell death[130]. However, apoptosis and necrotic cell death are the most characterized.

The expression ‘apoptosis’ has been coined by Kerr *et al.* [131] to describe a specific morphological aspect of cell death. Apoptosis is characterized by specific morphological and biochemical changes of dying cells, including cell shrinkage (pyknosis), nuclear condensation and fragmentation (karyorrhexis), dynamic membrane blebbing (but

maintenance of its integrity until the final stages of the process) and loss of adhesion to neighbours or to extracellular matrix [131]. Biochemical changes include chromosomal DNA cleavage into internucleosomal fragments, phosphatidylserine externalization and a number of intracellular substrate cleavages by specific proteolysis [132,133].

Mitochondria have a central role in regulating the apoptotic process because many apoptogenic proteins such as cytochrome c, apoptosis-inducing factor (AIF), caspases and so on, normally present in these organelles, are released following apoptotic damage and amplify the apoptotic process. This event is highly regulated through specific interactions between proteins of the Bcl-2 family. In this family, effector proteins such as Bax and Bak are essential to the machinery allowing membrane permeabilization. On the other hand, anti-apoptotic members such as Bcl-2 and Bcl-xL, inhibit this process by directly binding to the pro-apoptotic effectors. Finally, BH3-only proteins such as Bad or truncated Bid relay apoptotic stimuli to the mitochondria by interacting with both effectors and anti-apoptotic Bcl2 family members. Therefore, when challenged by an apoptotic stimulus, the combined signaling within the Bcl-2 family dictates the immediate fate of the cell, i.e., whether or not to induce permeabilization of the outer membrane. This phenomenon has been coined Mitochondrial Outer Membrane Permeabilization, or MOMP, and the released cytochrome c leads to an activation of the executioner caspases by proteolysis and eventually to plasma membrane blebbing. Cytochrome c release during MOMP typically occurs through the mitochondrial apoptosis-induced channel MAC.

'Necrotic cell death' or 'necrosis', instead, is morphologically characterized by a gain in cell volume (oncosis), swelling of organelles, plasma membrane rupture and subsequent loss of intracellular contents. For a long time, necrosis has been considered merely as an accidental uncontrolled form of cell death, but evidence is accumulating that the execution of necrotic cell death may be finely regulated by a set of signal transduction pathways and catabolic mechanisms [134,135]. For instance, death domain receptors (e.g., TNFR1, Fas/CD95 and TRAIL-R) and Toll-like receptors (e.g., TLR3 and TLR4) have been shown to elicit necrosis, in particular in the presence of caspase inhibitors.

In recent years, the role of the mitochondria in necrotic cell death has received considerable attention. Indeed, an increase of mitochondrial membrane permeability is one of the key events in apoptotic or necrotic death. The mitochondrial membrane permeability transition (MPT) is a Ca^{2+}-dependent increase of mitochondrial membrane permeability that leads to loss of $\Delta\Psi$, mitochondrial swelling, and rupture of the outer mitochondrial membrane. The MPT is thought to occur after the opening of a channel that is known as the permeability transition pore (PTP), which putatively consists of the voltage-dependent anion channel

(VDAC), the adenine nucleotide translocator (ANT), cyclophilin D (Cyp D: a mitochondrial peptidyl prolyl-cis, trans-isomerase), and other molecule(s).

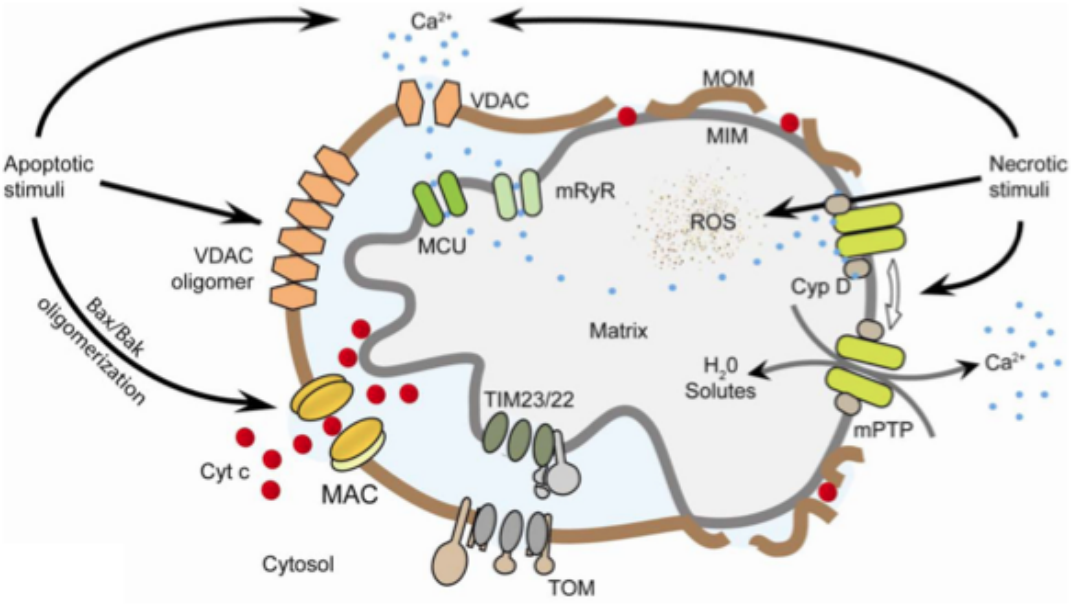

Figure 4. Left, Apoptotic stimuli induce relocation of Bax from the cytosol into the mitochondrial outer membrane (MOM). Bax, Bak, and possibly other unidentified protein(s) oligomerize and form MAC to release cytochrome c. VDAC oligomerization upon apoptotic stimuli was also reported to be involved in cytochrome c release. Right, Necrotic stimuli lead to exacerbated calcium uptake and reactive oxygen species generation by mitochondria. High levels of calcium and reactive oxygen species (ROS) induce a cyclophilin-D (Cyp D)- sensitive opening of mPTP that leads to swelling of the matrix and release of calcium. Swelling disrupts the outer membrane while released calcium activates proteases, phosphatases and nucleases that lead to necrotic degradation [136].

The involvement of the mPTP in necrosis and ischemia/reperfusion injury of the heart is a particularly well documented case [137]. Examination of cyclophilin-D-deficient mice has provided even more compelling evidence that the mPTP plays a crucial role in necrosis [138-140].

These data indicate that mPTP opening is chiefly involved in necrosis rather than in triggering cytochrome c release during early apoptosis. Nevertheless, MAC and mPTP opening may act alone or in combination, depending on cell type and death stimulus, to amplify the death signals. In this context, the swelling precipitated by mPTP opening would cause a remodeling of the cristae, which could facilitate a more complete release of cytochrome c and other pro-apoptotic factors from the mitochondria [141,142].

Therefore, the fate of the cell after an insult could depend on the extent of MPT. If MPT occurs to only a slight extent, the cell may recover, whereas if it progresses the cell may

undergo apoptosis. If it occurs to an even larger degree the cell is likely to undergo necrotic cell death [143].

2. AIM OF THE THESIS

SIRT3 is one of the most studied sirtuins and is involved in the regulation of many processes. It localizes in the mitochondria, one of the most important organelle of the cell. Indeed, mitochondria are responsible, among other things, for the energetic state of the cell and play a fundamental role in the cellular response toward stress condition. Several works point the attention on the role of SIRT3 in mediating cellular resistance toward various forms of stress by maintaining genomic stability and mitochondrial integrity.

Aim of the present study was to clarify the role of SIRT3 in the cellular response toward stress condition. In particular the role of SIRT3 in the presence of hypoxic and staurosporine (STS)-mediated stress was analyzed. Moreover the molecular mechanism by which this sirtuin confers resistance to cell death was investigated.

3. MATERIALS AND METHODS

3.1 Cell cultures

The MDA-MB-231 human breast carcinoma cell line, the human epithelial carcinoma cell line Hela and the human chronic myelongenous leukemia cell line K562 were purchased from LGC Standards (Milan, Italy). MDA-MB-231, Hela and K562 were maintained in 75-cm^2 polystyrene flasks (Corning Costar Corp., Oneonta, NY) with RPMI 1640 medium (Mediatech, Inc., Herndon, VA), containing 100 units/ml penicillin, 0,1 mg/ml streptomycin, and 10% heat-inactivated fetal bovine serum. Cells were maintained at 37°C in a humidified atmosphere of 5% CO_2 and 95% air.

3.2 Treatment Protocols and Antibodies

Hypoxia was achieved by incubating cells in a hypoxic chamber (Billups-Rothenberg Inc., Del Mar, CA) where a 1% oxygen mix was flushed in for 4 minutes according to the manufacturer's instructions.

Staurosporine (Sigma Aldrich, St Louis, MO, USA) was dissolved in dimethyl sulfoxide (DMSO) as 1mM stock solution and added to a final concentration of 250 nM.

Cyclosporin A (Biomol Research Laboratories, Plymouth Meeting, PA, USA) was dissolved in dimethyl sulfoxide and added at a final concentration of 5 μM.

NAC (Sigma Aldrich) was dissolved in RPMI and added at a final concentration of 5 mM.

The following primary antibodies were used: rabbit anti-SIRT3 antibody, rabbit anti-AIF (Cell Signaling Technology, Inc., Danvers, MA, USA), mouse anti-HIF-1a, mouse anti-laminin (BD Bioscience, San Jose, CA, USA), mouse anti-cytochrome c, mouse anti-prohibitin, rabbit anti-SP1, rabbit anti-CA IX and mouse anti-CA VB (Novus Biologicals, Littleton, CO, USA), mouse anti-β actin, rabbit anti-Bax (N-20), goat anti HKII, mouse anti-PARP (Santa Cruz Biotechnology, Santa Cruz, CA, USA) and rabbit anti-HMGB1 (Sigma-Aldrich).

The following secondary antibodies were used: mouse anti-rabbit HRP, goat anti-mouse HRP (Amersham Biosciences, Piscataway, NJ, USA) and donkey anti-goat HRP (Santa Cruz Biotechnology).

3.3 Generation of stable SIRT3 transfectants

MDA-MB-231 cells were stably transfected with a pcDNA3.1 expression vector encoding for human SIRT3-Flag (Addgene Inc., Cambridge, MA). Stable clones were generated by delivering plasmid DNA constructs into cells using TurboFectin 8.0 (Origene Technologies, Rockville, MD) according to the manufacturer's recommendations. Briefly, cells were seeded on a 24 well plate. The following day the cells were transfected. Turbofectin reagents were first mixed with serum free RPMI at room temperature for 5 minutes. Subsequently plasmid DNA was added to the TurboFectin-containing media and incubated at room temperature for 30 minutes. After that, the mixtures were added to the cells. The selection of stable clones was started 24h later with the addition of 500 μg/ml of Geneticin (Sigma-Aldrich, St Louis, MO).

3.4 Lentiviral transduction

MissionTM TRC short hairpin RNA (shRNA) lentiviral transduction particles expressing short hairpin RNA (shRNA) targeting SIRT3, SP1, HIF-1α and lentiviral negative control particles were purchased from Sigma-Aldrich. Stably transduced clones were generated according to the manufacturer's instructions. Briefly, cells were seeded on a 24 well plate. The following day cells were infected. After 24h medium was changed with fresh RPMI. Selection of stable clones was started 24h later with the addition of 3 μg/ml of puromycin. The expression of SIRT3, SP1, HIF-1α was confirmed by Western blotting.

3.5 Annexin V/Propidium iodide (PI) staining

To discriminate between apoptotic and necrotic cell death and to study the effect of SIRT3 on these processes dual staining with fluorescent Annexin V and propidium iodide (PI) was performed. Annexins are a family of calcium-dependent phospholipid-binding proteins, which bind to phosphatidylserine (PS) to identify apoptotic cells. In healthy cells, PS is predominantly located along the cytosolic side of the plasma membrane. Upon initiation of apoptosis, PS loses its asymmetric distribution in the phospholipid bilayer and translocates to the extracellular membrane, which is detectable with fluorescently labeled Annexin V. In early stages of apoptosis, the plasma membrane excludes PI and therefore cells which display only Annexin V staining (PI negative) are in early stages of apoptosis. During late-stage apoptosis or in cells undergoing necrosis, loss of cell membrane integrity allows Annexin V binding to cytosolic PS, as well as cell uptake of PI.

Cells (2 x 10^6) were plated in 100 mm dishes. Following treatment the cells were washed twice in PBS, collected and centrifuged at 2000 rpm for 10 min at 4°C. Percentage of apoptotic and necrotic cells was quantified with the FITC Annexin V apoptosis detection kit I (BD Bioscience) according to manufacturer's recommendations. Briefly, cell pellets were resuspended in 1 ml of 1X binding buffer and 100 µl of the suspension were transferred in a 5 ml tube. FITC Annexin V (5 µl) and PI (5 µl) were added to the cells for 15 minutes at room temperature. Afterward, 400 µl of 1X binding buffer were added to each tube and analyzed with a FACSCalibur (BD Biosciences, San Jose, CA) flow cytometer.

3.6 Hoechst staining

Cells were seeded on glass coverslips in a 6 well plate. Following treatment nuclei were stained by addition of Hoechst (Sigma-Aldrich) staining solution at a final concentration of 62.5 ng/ml. After 15 minutes incubation cells were washed twice and fixed in 3.7% paraformaldehyde for 10 min. After two washes in PBS, coverslips were mounted and stained nuclei observed under fluorescence microscope (Carl Zeiss, Milan, Italy).

3.7 Isolation of Nuclear, Cytosolic and Mitochondrial Fractions

Cells (2 x 10^6) were plated in 100 mm dishes. Following treatment the cells were scraped off the plate using a rubber policeman and centrifuged at 2000 rpm for 10 min at 4°C. The cell pellets were resuspended in 1 ml of 20 mM HEPES-KOH, pH 7.5, 10 mM KCl, 1.5 mM $MgCl_2$, 1 mM EDTA, 1 mM EGTA, 1 mM phenylmethylsulfonyl fluoride, 10 µg/ml leupeptin, 10 µg/ml aprotinin, and 250 mM sucrose. The cells were broken open with six passages through a 26-gauge needle applied to a 1-ml syringe. The homogenate was centrifuged at 1000 g for 5 min at 4°C to harvest nuclei. The supernatant was transferred to a high-speed centrifuge tube and centrifuged at 10000 g for 25 min at 4°C. The resulting supernatant (cytosolic fraction) was concentrated through a Microcon YM-10 Centrifugal Filter Device (Millipore, Bedford, MA), while the pellet (mitochondrial fraction) was lysed in 50 mM Tris [tris(hydroxymethyl)aminomethane]–HCl, 150 mM NaCl, 1% Triton X-100, 0,1% Nonidet P-40, 1 mM phenylmethylsulfonyl fluoride, 10 µg/ml leupeptin, 10 µg/ml aprotinin). Protein concentration of the fraction was determined by the Bradford assay (Bio-Rad, Hercules, CA). For all experiments, the purity as well as equal loading of nuclear fraction was determined by measuring levels of nuclear protein lamin. The purity as well as

equal loading of mitochondrial fraction was determined by measuring levels of mitochondrial protein prohibitin (phb). The purity as well as equal loading of cytosolic fraction was determined by measuring levels of cytosolic protein β-actin.

3.8 Protein extraction and Western Blot Assay

Cells (1 x 10^6) for whole cell lysate were pelleted at 700 x g (5 min at 4°C) and lysed in 50 µl of cell lysis buffer (20 mM Tris, pH 7.4, 100 mM NaCl, 1% Triton, 1 mM phenylmethylsulfonyl fluoride, 10 µg/ml leupeptin, 10 µg/ml aprotinin). After 30 min on ice, the lysates were clarified by centrifugation (10 min at 4°C) and the supernatant collected. Protein concentration was determined by the Bradford assay (Bio-Rad, Hercules, CA). Equivalent amounts of protein were electrophoresed on SDS-polyacrylamide gels. Kaleidoscope Prestained Standards (Bio-Rad) were used to determine molecular weight. The gels were then electroblotted onto PVDF membranes. After blocking with 5% milk, membranes where incubated with the primary antibody overnight. Finally, the relevant protein was visualized by staining with the appropriate secondary horseradish peroxidase-labeled antibody for 1 hour followed by enhanced chemiluminescence.

3.9 Measurement of the Mitochondrial Membrane Potential

The change in mitochondrial membrane potential ($\Delta\Psi_m$), was analyzed by flow cytometry using the $\Delta\Psi_m$ sensitive dye 5,5',6,6'-tetrachloro-1,1',3,3'-tetraethylbenzimidazolylcarbocyanine iodide (JC-1). The $\Delta\Psi_m$ is an important parameter of mitochondrial function used as an indicator of cell health. JC-1 is a lipophilic, cationic dye that can selectively enter into mitochondria and reversibly change color from red to green as the membrane potential decreases. In healthy cells with high mitochondrial $\Delta\Psi_m$, JC-1 spontaneously forms complexes known as J-aggregates with intense red fluorescence. On the other hand, in apoptotic or unhealthy cells with low $\Delta\Psi_m$, JC-1 remains in the monomeric form, which shows only green fluorescence. The ratio of green to red fluorescence is dependent only on the membrane potential and not other factors such as mitochondrial size, shape, and density, which may influence single-component fluorescence signals.

To perform this assay the cells (1 x 10^4 for normoxic condition and 6 x 10^4 for hypoxic condition) were cultured in 24-well plate. Following treatment cells were harvested by

centrifugation at 1000 rpm for 5 min at room temperature. The cell pellets were resuspended in 0,5 ml of cell culture media containing 10 μM JC-1, incubated for 15 min at 37 °C in 5% CO_2 and immediately transferred on ice. Cell staining was determined by FACSCalibur (BD Biosciences, San Jose, CA). Two light-scattering parameters, the forward scatter (FSC; cell size) and side scatter (SSC; intracellular granularity and complexity), and two fluorescence parameters, fluorescence channel 1 (FL1) and fluorescence channel 2 (FL2), were measured.

3.10 Measurement of intracellular reactive oxygen species (ROS)

To determine the amount of ROS production, 2',7'-dichlorodihydrofluorescin-diacetate (DCFH-DA) was used. The probe is loaded into the cells to provide a readily oxidizable substrate. DCFH-DA is lipophilic and easily crosses cell membrane. Inside the cell, cytosolic esterases deacetylate the probe to form polar, non fluorescent 2'-7'-dichlorodihydrofluorescin (DCFH) which, due to it polarity is trapped either within the cytoplasm or in myeloperoxidase (MPO)-positive intracellular granules. The oxidative potential of intracellular ROS are able to oxidize the trapped DCFH to 2'-7'-dichlorodihydrofluorescein (DCF), whose green fluorescence at 525 nm is easily measurable on the flow cytometer. The fluorescence intensity is proportional to the ROS levels within the cell cytosol. Briefly following treatment cells were harvested by centrifugation at 1200 rpm for 5 min at room temperature. The pellets were resuspended in 0,5 ml of cell culture media containing 50 μM DCFH-DA and incubated for 30 minutes at 37°C in 5% CO_2. Fluorescence intensity was measured by flow cytometer (FACScalibur, BD Biosciences, San Jose, CA) using excitation and emission wavelengths of 480 nm and 530 nm, respectively.

3.11 Carbonic Anhydrase activity measurements

CA catalytic activity was determined using a slightly modified end-point titration method of Maren. (37) Briefly, intact cell (for CA IX activity) or mitochondrial extracts (for CA VB activity) were resuspended in 500 μl of ice-cold assay buffer (20 mM imidazole, 5 mM Tris, 0,2 mM p-nitrophenol). The cuvette containing the sample and assay buffer was placed in a Lambda 35 UV/VIS (Perkin Elmer Instruments, Waltham, MA, USA) spectrophotometer and 500 μl of ice-cold CO2-saturated H2O was added into the cuvette.

The exact time in seconds for the yellow color disappearance was counted. In the control experiments without cells or extracts, the color disappeared in about 75 sec.

3.12 Intracellular and extracellular pH determination

The effect of SIRT3 expression on cytosolic pH was evaluated by flow cytometry using the pH sensitive fluorescent probe 2′,7′-Bis(2-carboxyethyl)-5(6)-carboxyfluorescein acetoxymethyl ester (BCECF-AM) (Sigma Aldrich). Following treatment cells were harvested by centrifugation and the pellets were resuspended in RPMI 1640 medium containing 20 μmol/l BCECF-AM and incubated for 30 min at 37°C in 5% CO_2. The cells were then washed in HBSS, placed on ice and analyzed with a FACSCalibur equipped with 488 nm argon laser collecting the emission of BCECF-AM in the FL1 and FL2 channels. The relative cytosolics pH of individual cells was displayed in the two-dimensional dot-plot showing the fluorescence intensity at 520 nm (FL1, base) and 640 nm (FL2, acid) as described in details previously [144]. To obtained a calibration curve, about 10^7 cells were kept at 37% °C for 30 min in 1 ml RPMI 1640 medium containing 20 mmol/l BCECF-AM and later incubated with different potassium phosphate buffers in a range of pH from 5.5 to 8 in the presence of nigericin (10 μmol/l).

Extracellular pH was determined in the culture medium with a pH211 pHmeter (Hanna Instruments, Milan, Italy).

3.13 Analysis of lactate production

Accumulation of lactate in the culture medium was determined using lactate assay kit (Biovision, Mountain View, CA) according to the manufacturer's protocol. Briefly, following treatment culture media was collected, concentrated and transferred in a 96-wells plate that already containing the reaction mixture. After 30 minutes of incubation at room temperature the absorbance of solution was measured at 450 nm by using a microplate reader. The assays were performed in triplicate, and the results, expressed as mean. The lactate concentration in the media was calculated according to the manufacturer's instruction.

3.14 Analysis of lactate dehydrogenase (LDH) activity

The activity of LDH was analyzed using the LDH Cytotoxicity Assay Kit II (BioVision, Mountain View, USA), and the assay was performed as described below. Following treatment culture media were collected after centrifugation at 600 g for 10 min, while cells were harvested by centrifugation at 1200 rpm for 5 min at room temperature and lysed with the Cell Lysis solution from the kit. The clear medium and the lysates were transferred into an optically clear 96-well plate that already containing the reaction mixture and incubated for 30 min at room temperature. Following incubation, the absorbance of solution was measured at 450 nm by using a microplate reader. The assays were performed in triplicate, and the results, expressed as mean. LDH levels in the media versus the cells were quantified and compared to the control values according to the manufacturer's instructions.

3.15 SIRT3 deacetylase activity assay

SIRT3 deacetylase activity was determined using a SIRT3 Fluorimetric Activity Assay/Drug Discovery Kit (Biomol Research Laboratories) following the manufacturer's protocol. In brief, the mitochondrial extract (5 mg) was incubated with the Fluor de Lys substrate buffer at 371C for 1h followed by incubation with fluor de lys developer at 37°C for 40min. After excitation at 360nm, emitted light was detected at 460nm using Infinte 200 microplate fluorometer (Tecan, Ma¨nnedorf, Switzerland). The fluorescence intensity of the assay buffer was subtracted from each experimental sample.

3.16 SIRT3 promoter construction and luciferase assay

The pGL2 plasmid containing the SIRT3 promoter region was gently donated by Dr. Bellizzi. The deletion analysis as well as luciferase assay were performed by the laboratory of Dr. Bellizzi.

3.17 Statistical analysis

The results are expressed as means ± S.D. and 95% confidence intervals (95% CI). Before using parametric tests, the assumption of normality was verified using the Shapiro–Wilk W-test. Student's paired t-test was used to determine any significant differences before and after treatment. Significance was set at 0.05 (Pr0.05). SPSS statistical software package

(SPSS Inc., Version 13.0.1 for Windows Chicago, IL, USA) was used for all statistical calculations.

4. RESULTS

4.1 SIRT3 protects cells from both apoptotic and necrotic cell death.

The protective role of SIRT3 in MDA-MB-231 and HeLa cells was evaluated by stably silencing or overexpressing this sirtuin (Figure 5A). SIRT3 activity in mitochondrial fractions of MDA-MB-231 and HeLa cells was increased in overexpressing and decreased in silenced cells compared with control untrasfected cells (Figure 5B).

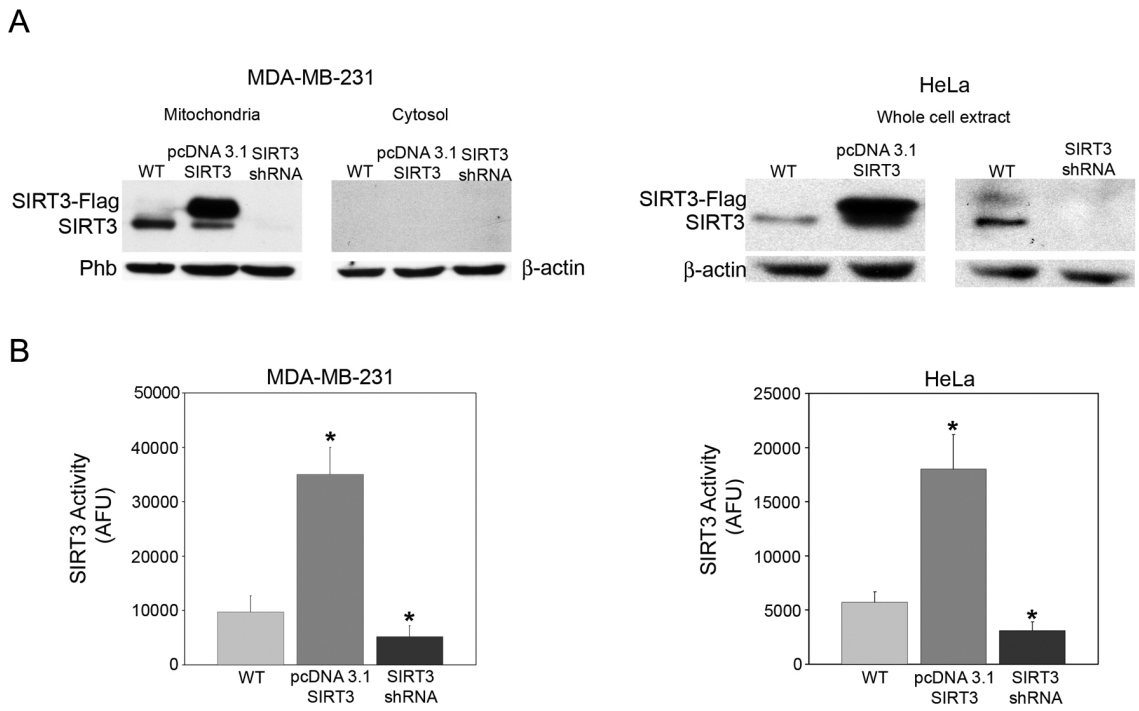

Figure 5. (A) SIRT3 was either overexpressed or silenced in MDA-MB-231 and in HeLa cells and stable clones obtained. SIRT3 content was determined on mitochondria and cytosol (MDA-MB-231) or whole lysates (HeLa) by Western blot. Data are representative of at least three separate experiments. Prohibitin (Phb) was used as loading control for mitochondria, whereas b-actin was used as a loading control for cytosol or whole lysates. **(B)** MDA-MB-231 and HeLa WT, SIRT3 overexpressing and SIRT3-silenced cells were processed to isolate mitochondrial fractions. SIRT3 activity was measured as described under Materials and Methods. Data are representative of at least three separate experiments. Values are represented as mean $\pm$ s.d. *, significantly different from WT. Significance was set at $P<0.05$.

Figure 6A shows percentage of cell death measured by propidium iodide (PI)/ Annexin V staining in WT, SIRT3-overexpressing or silenced cells treated with hypoxia or STS 250 nM for 48 h. Hypoxia was used to induce necrotic cell death, whereas STS was used to induce apoptosis. It is worth noting, however, that when treating cells with hypoxia or STS, we never observed a clear PI^+ population but always PI^+/Annexin V^+ cells. This is probably due, as also reported by Krisko et al. [145], to the externalization by necrotic cells of phosphatidylserine during hypoxia.

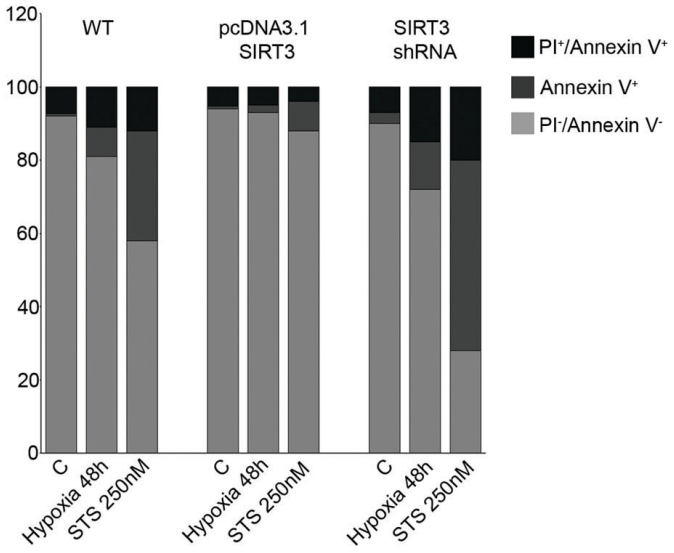

Figure 6. MDA-MB-231 WT, SIRT3 overexpressing and SIRT3-silenced cells were incubated under normoxia or hypoxia for 48h. Alternatively, cells were treated with STS 250 nM for 48h. Following treatment, cells were stained with PI and Annexin V as described under Materials and Methods. Percentages of PI^+/Annexin V^+ (necrotic), PI^-/Annexin V^+ (apoptotic) and PI^-/Annexin V^- (vital) cells are reported as bar graphs.

After 48 h of hypoxia, 11% of WT cells were PI^+/Annexin V^+, whereas 8% were PI^-/Annexin V^+ (Figure 6). Overexpression of SIRT3 reduced PI^+/Annexin V^+ cells to 2% and PI^-/Annexin V^+, to 5%. SIRT3 silencing increased PI^+/Annexin V^+ to 15% and PI^-/Annexin V^+ cells to 13%. In the presence of STS, PI^+/Annexin V^+ cells were 12, 4 and 20%, whereas PI^-/Annexin V^+ cells were 30%, 8% and 52% for WT, SIRT3-overexpressing and SIRT3-silenced cells, respectively (Figure 6). Images and percentage of cell killing after hypoxia and STS treatment are shown in Figure 7A. Moreover, images and total number of apoptotic nuclei counted after Hoechst staining are also reported in Figure 7B. Importantly, cyclosporin A (CsA), an inhibitor of the MPT pore [146] reduced SIRT3-silenced hypoxic cell death to a percentage similar to that of WT cells (Figure 7A and 7B). Similar results were obtained in WT, SIRT3-overexpressing and SIRT3-silenced HeLa cells exposed to hypoxia (Figure 8A). Interestingly, SIRT3 protection was observed also after 7 days of hypoxia when only 30% of SIRT3 overexpressing cells were killed (Figure 8B). By contrast, at the same time, 65% of WT cells and 90% of SIRT3-silenced cells were dead (Figure 8B).

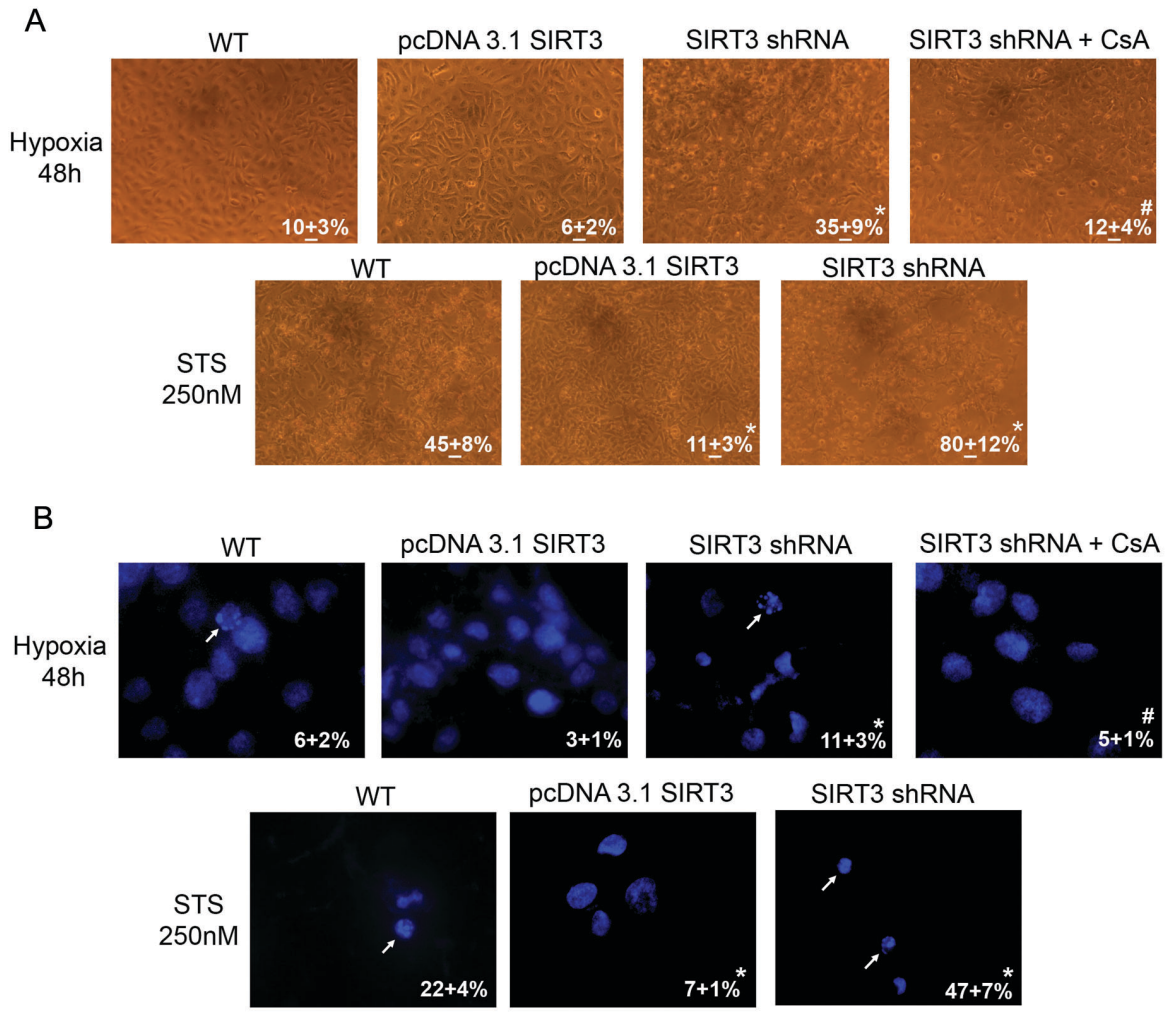

Figure 7. (A) MDA-MB-231 WT, SIRT3 overexpressing and SIRT3-silenced cells were incubated under normoxia or hypoxia for 48h. Furthermore, SIRT3-silenced cells were also incubated under hypoxia in the presence of CsA 5 μM. Alternatively, MDA-MB-231 WT, SIRT3 overexpressing and SIRT3-silenced cells were treated with STS 250 nM for 48h. Pictures of the cells were taken at 20x with a digital camera mounted on an EclipseNet 2000 microscope. Percentage of cell death was determined by Trypan blue exclusion. Values are represented as mean + s.d. *, significantly different from WT. #, significantly different from SIRT3-silenced cells. Significance was set at $P<0.05$. **(B)** MDA-MB-231 WT, SIRT3 overexpressing and SIRT3-silenced cells were incubated under normoxia or hypoxia for 48h. Furthermore, SIRT3-silenced cells were also incubated under hypoxia in the presence of CsA 5 μM. Alternatively, MDA-MB-231 WT, SIRT3 overexpressing and SIRT3-silenced cells were treated with STS 250 nM for 48h. Following treatment cells were stained with Hoechst as described under "Materials and Methods". Pictures of apoptotic nuclei were taken at 60x with an AxioCam digital camera mounted on a Zeiss LSM 510 fluorescent microscope. Apoptotic and intact nuclei from 5 different fields for a total of 150 cells were counted and values reported in each image. Values are represented as mean + s.d. *, significantly different from WT. #, significantly different from SIRT3-silenced cells. Significance was set at $P<0.05$. Apoptotic nuclei are indicated by white arrows.

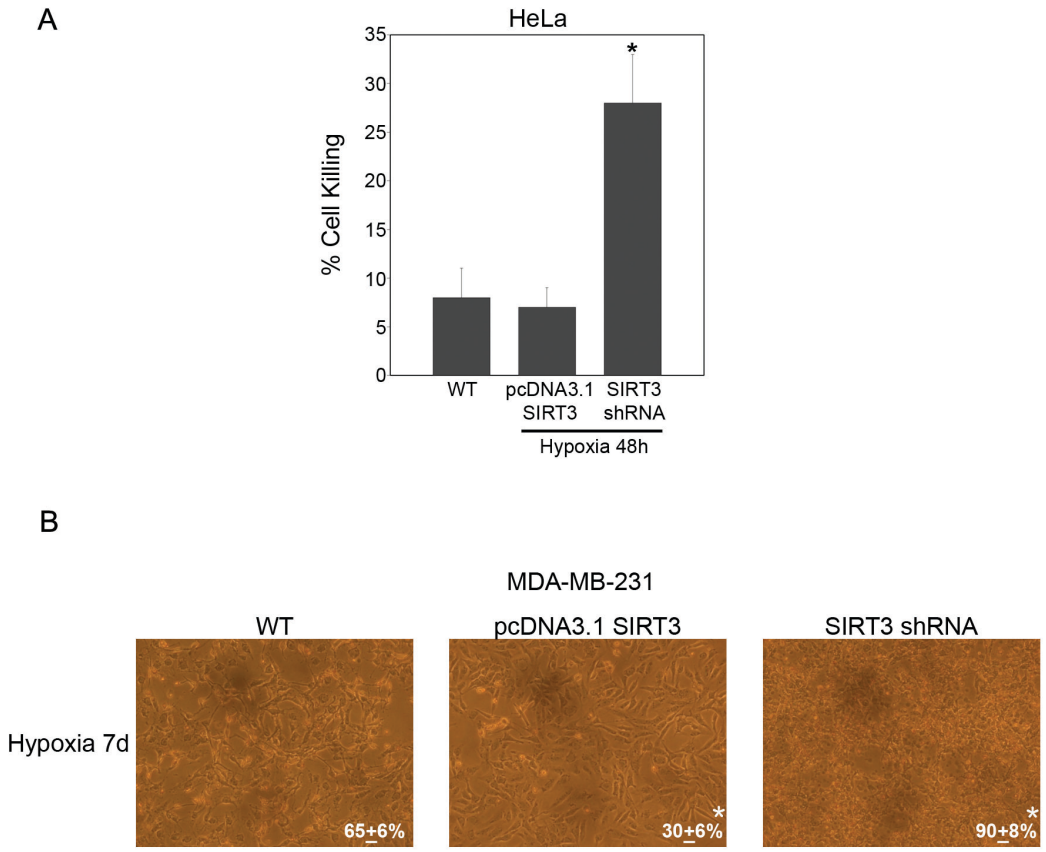

Figure 8. (A) HeLa WT, SIRT3 overexpressing and SIRT3-silenced cells were incubated under normoxia or hypoxia for 48h. Percentage of cell killing was determined by trypan blue exclusion as described under Materials and Methods. Values are represented as mean ± s.d. *, significantly different from control normoxic cells. Significance was set at $P<0.05$. **(B)** MDA-MB-231 WT, SIRT3 overexpressing and SIRT3-silenced cells were incubated under normoxia or hypoxia for 7 days. Pictures of the cells were taken at 20x with a digital camera mounted on an EclipseNet 2000 microscope. Percentage of cell death was determined by Trypan blue exclusion. Values are represented as mean ± s.d. *, significantly different from WT. Significance was set at $P<0.05$.

In our model, we assessed, in the extracellular medium, lactate dehydrogenase (LDH) as an accurate measure of cell membrane integrity and cell death, and high mobility group box 1 (HMGB1) protein release as an accurate measure of necrotic cell death [145]. In fact, HMGB1 is a DNA-associated protein that remains bound to DNA during apoptosis, being released only by necrotic cells [145]. Figure 9A shows that 72 h of hypoxia significantly increased LDH release in WT cells. Overexpression of SIRT3 reduced LDH release, whereas SIRT3 silencing caused a burst in LDH released into the culture medium (Figure 9A). Figure 9B shows that WT cells released HMGB1 after 72 h of hypoxia. By 6 days of hypoxia, there was a clear accumulation of HMGB1. SIRT3-over-expressing cells showed a reduced accumulation of HMGB1 in the extracellular medium both at 72h and 6 days (Figure 9B).

By contrast, SIRT3-silenced cells showed HMGB1 release under normoxia that was significantly increased after 72 h and 6 days of hypoxia (Figure 9B).

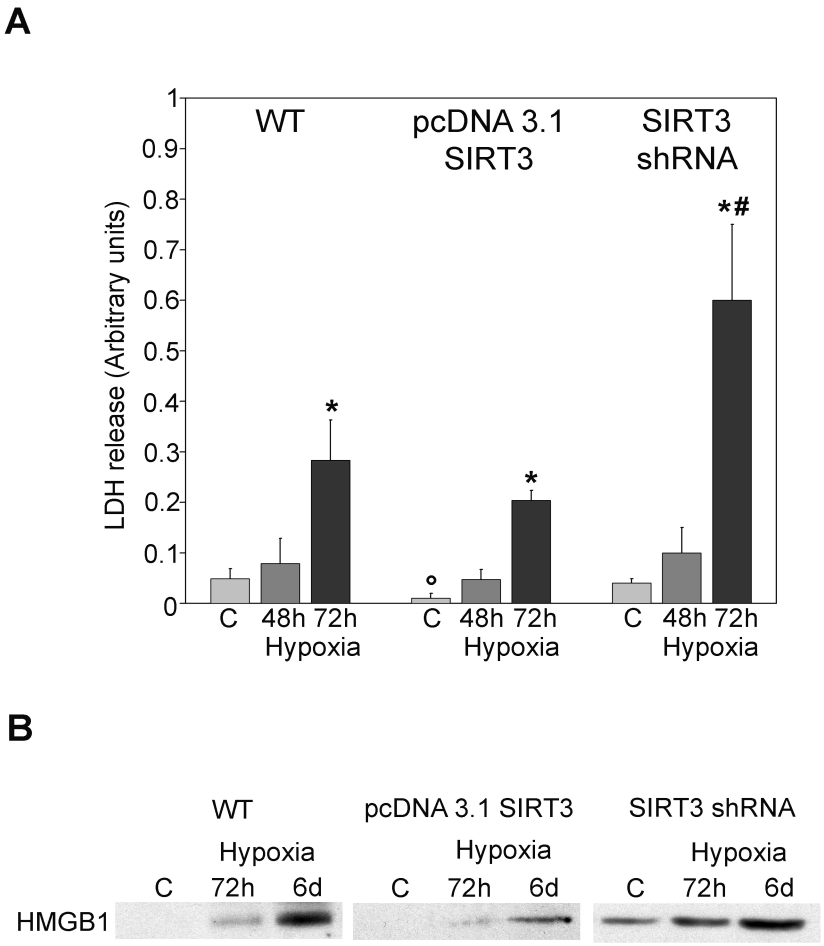

Figure 9. **(A)** MDA-MB-231 WT, SIRT3-overexpressing and SIRT3-silenced cells were incubated under normoxia, hypoxia for 48 and 72 h. Activity of LDH released by the cells was measured as described under Materials and Methods. *Significantly different from control normoxic and hypoxia 48 h. 1Significantly different from control WT and SIRT3- silenced cells. # Significantly different from 72h hypoxia of WT and SIRT3- overexpressing cells. Significance was set at $P<0.05$. **(B)** MDA-MB-231 WT, SIRT3-overexpressing and SIRT3-silenced cells were incubated under normoxia, hypoxia for 72 h and 6 days. Afterward, cellular medium was collected. HMGB1 extracellular levels were determined by western Blot. C, control normoxic cells

4.2 SIRT3 effects on $\Delta\Psi_{mt}$ and pH_i.

MPT induction with loss of $\Delta\Psi_{mt}$ is considered a key event in the control of apoptotic and necrotic cell death [147]. The effects of SIRT3 on $\Delta\Psi_{mt}$ was evaluated in WT, SIRT3-overexpressing and SIRT3-silenced cells. Figure 10 shows that under normoxia 8% of WT cells had a low $\Delta\Psi_{mt}$. By contrast, about 25% of SIRT3-silenced cells had a low $\Delta\Psi_{mt}$

under the same conditions (Figure 10). Interestingly, only 4% of SIRT3-overexpressing cells showed a low $\Delta\Psi_{mt}$ (Figure 10). The number of cells with reduced $\Delta\Psi_{mt}$ increased after 24 h of hypoxia. In fact, Figure 10 also shows that 20% of WT cells had a low $\Delta\Psi_{mt}$ when under hypoxia. Such a percentage was 10% in SIRT3-overexpressing cells and 43% in SIRT3-silenced cells (Figure 10). Similarly, STS caused $\Delta\Psi_{mt}$ loss in 25% of WT, 12% of SIRT3-overexpressing and 27% of SIRT3-silenced cells (Figure 10).

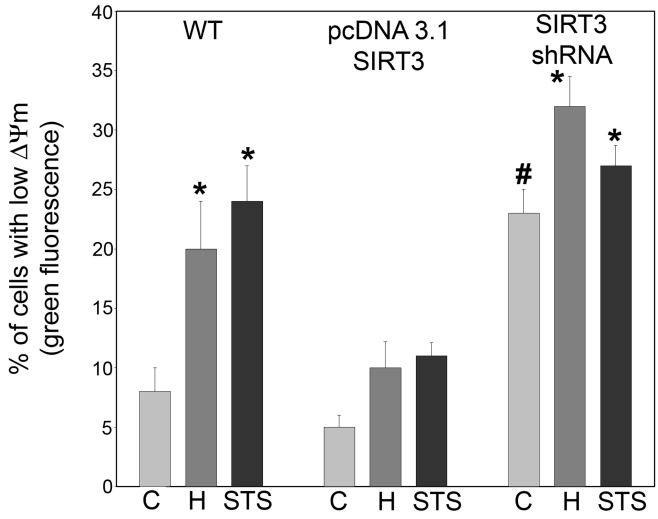

Figure 10. MDA-MB-231 WT, SIRT3-overexpressing and SIRT3-silenced cells were incubated under normoxia, hypoxia or STS for 24 h. Changes in $\Delta\Psi_{mt}$ were determined by using the $\Delta\Psi_{mt}$ sensitive dye JC-1. Fluorescence intensity was measured by flow cytometry as described under Materials and Methods. Data are representative of at least three separate experiments. Values are represented as mean±S.D. * Significantly different from control normoxic cells. # Significantly different from control normoxic cells of WT and SIRT3-overexpressing clones. Significance was set at $P < 0.05$.

Mitochondria are the main source of ROS and SIRT3 has been shown to modulate the activity of crucial enzymes involved in ROS scavenging [102]. Therefore, ROS production was measured in WT and SIRT3 clones. Figure 11 left side shows that 48 h of hypoxia treatment increased intracellular ROS in WT cells, an effect reduced by the ROS scavenger N-acetyl-cysteine (NAC). Overexpression of SIRT3 reduced both basal and hypoxia-induced accumulation of ROS (Figure 11 left side). By contrast, SIRT3 silencing significantly increased ROS accumulation with only a partial reduction by NAC (Figure 11 left side). Interestingly, NAC also reduced SIRT3 expression in WT cells under both normoxic and hypoxic conditions (Figure 11 right side).

Maintenance of pH_i within the physiological range is important because of its effect on a number of enzymes, on the efficiency of the contractile elements, on ion channels and on the cell cycle [148]. Alteration of pH_i affects metabolic enzymes activity, protein synthesis as

well as many other cellular processes[148].

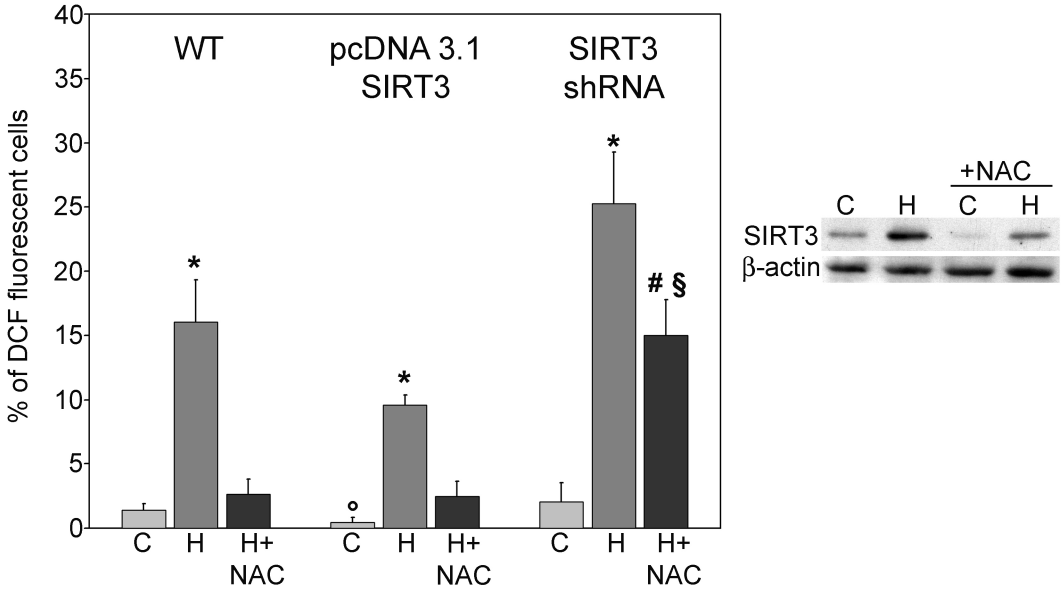

Figure 11. Left side, MDA-MB-231 WT, SIRT3 overexpressing and SIRT3-silenced cells were incubated under normoxia, hypoxia or hypoxia plus NAC for 48h. Intracellular ROS levels were determined by using 2',7'-dichlorfluorescein-diacetate (DCFH-DA). Fluorescence intensity was measured by flow cytometry as described under Materials and Methods. Data are representative of at least three separate experiments. Values are represented as mean ± s.d. *, significantly different from control cells. °, significantly different from control WT and SIRT3-silenced cells. #, significantly different from hypoxia + NAC of WT and SIRT3 overexpressing cells. §, significantly different form SIRT3-silenced control cells. Significance was set at $P<0.05$. Right side, MDA-MB-231 cells were incubated under normoxia or hypoxia for 48h in the presence or absence of NAC. SIRT3 levels were measured by Western blot (right side). b-actin was used as a loading control. Blots are representative of at least three separate experiments. C: control normoxic cells. H: hypoxic cells.

We observed that acidification of the growth medium was accelerated in SIRT3-silenced cells compared with WT or SIRT3-overexpressing cells. For this reason we proceeded by measuring both intracellular and extracellular pH. Figure 12A shows that SIRT3 silencing caused a significant drop in pH_i that was more evident under hypoxia. WT cells showed a decrease in pH_i after 48h of hypoxia treatment. By contrast, no intracellular acidification was observed in SIRT3-overexpressing cells (Figure 12A). Finally, increased proton production and extrusion was measured by determining culture medium acidification following 24 and 48h of hypoxia. Figure 12B shows that hypoxia increased extracellular acidification in SIRT3-silenced cells compared with WT cells. By contrast, SIRT3 overexpression prevented extracellular acidification (Figure 12B).

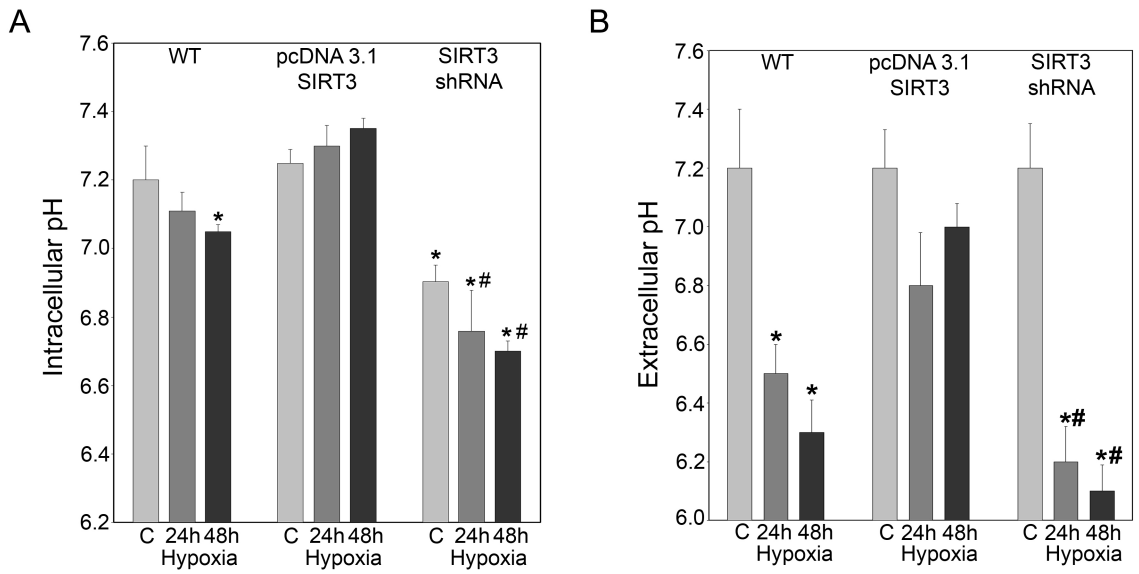

Figure 12. (A) MDA-MB-231 WT, SIRT3-overexpressing and SIRT3-silenced cells were incubated under normoxia or hypoxia for 24 and 48 h. pH_i was evaluated by flow cytometry using the pH-sensitive fluorescent probe BCECF-AM as described under Materials and Methods. Data are representative of at least three separate experiments. *Significantly different from control normoxic WT and SIRT3-overexpressing cells. #Significantly different from control SIRT3-silenced cells and from hypoxia-treated WT and SIRT3-overexpressing cells. Significance was set at $P<0.05$. **(B)** MDA-MB-231 WT, SIRT3-overexpressing and SIRT3-silenced cells were incubated under normoxia or hypoxia for 24 and 48 h. Extracellular pH in culture medium was determined as described under Materials and Methods. *Significantly different from control normoxic cells. #Significantly different from hypoxia of WT and SIRT3-overexpressing cells. Significance was set at $P<0.05$. C, control normoxic cells.

4.3 SIRT3 effects on HKII mitochondrial binding and carbonic anhydrase (CA) activity.

In order to unravel the mechanisms involved in the alterations of intracellular and extracellular pH that we observed following SIRT3 over-expression or silencing, we focused our attention on HKII and CA enzymes. Our choice is motivated by the fact that SIRT3 has been shown to modulate HKII binding to the outer mitochondrial membrane (OMM), thereby regulating both the opening/closing of the permeability transition pore (PTP) and the glycolytic rate [96,146]. Figure 13A shows that hypoxia increased HKII expression. In fact, the decrease observed after 72h of hypoxia in SIRT3-silenced cells is probably due to the increasing cell death rate. Next, we measured HKII content in the mitochondrial and cytosolic fractions from WT and SIRT3 clones (Figure 13A). In WT cells, HKII accumulated in the mitochondrial fraction. However, in SIRT3-overexpres- sing cells such an accumulation was absent during the first 36h of hypoxia when HKII was mostly cytosolic. After 72h of hypoxia we observed some HKII mitochondrial translocation (Figure 13A). By contrast, SIRT3-silenced cells had a high HKII content in the mitochondria under normoxia that did not change after 36h of hypoxia (Figure 13A).

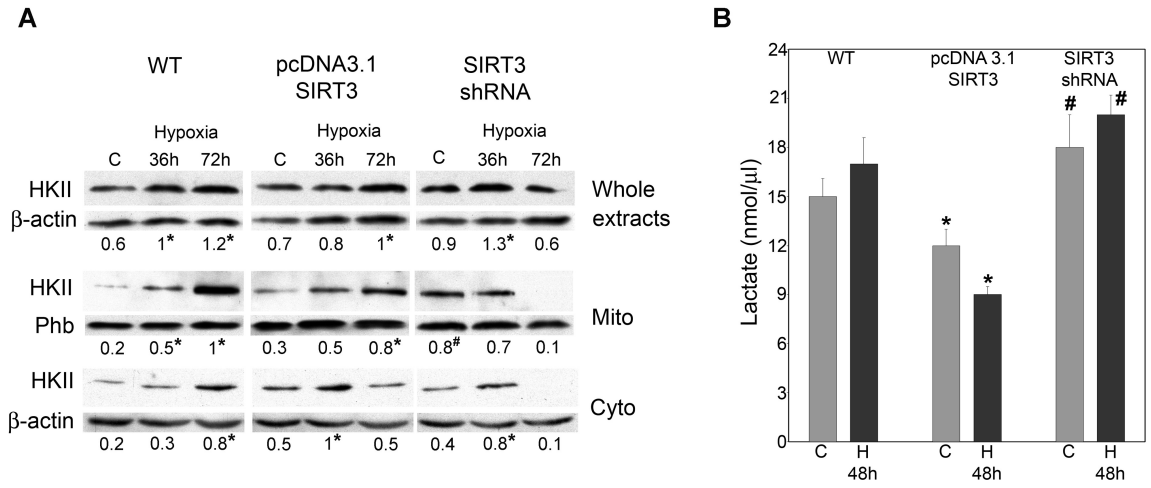

Figure 13. (A) MDA-MB-231 WT, SIRT3-overexpressing and SIRT3-silenced cells were incubated under normoxia or hypoxia for 36 and 72 h. Whole extracts or mitochondrial and cytosolic fractions were obtained. HKII content was measured as described under Materials and Methods. Data are representative of at least three separate experiments. Phb was used as loading control for mitochondria, whereas b-actin was used as a loading control for cytosol. Numbers below each blot represent average HKII level relative to either Phb or b-actin. *Significantly different from control normoxic cells (C). #Significantly different from control normoxic WT and SIRT3-overexpressing cells. Significance was set at $P<0.05$. **(B)** MDA-MB-231 WT, SIRT3-overexpressing and SIRT3-silenced cells were incubated under normoxia or hypoxia for 48 h. Lactate accumulation in culture medium was measured as described under Materials and Methods. *Significantly different from normoxia and hypoxia 48 h of WT and SIRT3-silenced cells. #Significantly different from normoxia and hypoxia of WT and SIRT3-overexpressing cells. Significance was set at $P<0.05$. C: control normoxic cells.

Increase in glycolytic rate was measured through the lactate released in the cellular medium. Figure 13B shows that both normoxic and hypoxic SIRT3-overexpressing cells released less lactate compared with WT cells. By contrast, SIRT3-silenced cells had an increased accumulation of lactate in the extracellular medium both under normoxia and hypoxia (Figure 13B).

To our knowledge, no data have been published on SIRT3 and CA. However, CA is an enzyme that has been shown to have a major role in the control of pH_i[149]. CA catalyzes the reversible reaction: $CO_2 + H_2O$ -- $H^+ + HCO_3^-$. In mammals, 16 CA isoforms have been discovered so far. Among these, the hypoxia-induced CA IX has a plasma membrane localization, whereas the less-studied CA VB localizes to the mitochondrial matrix where it controls $CO2/HCO3^-$ balance and Krebs cycle stimulation [149]. Hypoxia incubation of WT and SIRT3-overexpressing cells significantly increased CA IX expression and activity (Figures 14A and B). In SIRT3-silenced cells there was a significant increase of CA IX in normoxic cells, that was also accompanied by an increased catalytic activity (Figures 14A and B). Again, hypoxia stimulated CA IX synthesis and activity (Figures 14A and B). SIRT3 and CA VB are both localized in the mitochondrial matrix; therefore, we examined CA VB expression. Figure 14C shows that hypoxia did not significantly increase CA VB

levels. However, in WT cells, hypoxia increased CA VB catalytic activity (Figure 14D). Interestingly, SIRT3 overexpression significantly increased CA VB catalytic activity both under normoxia and hypoxia compared with WT and silenced cells. By contrast, in SIRT3-silenced cells, CA VB catalytic activity was significantly reduced (Figure 14D).

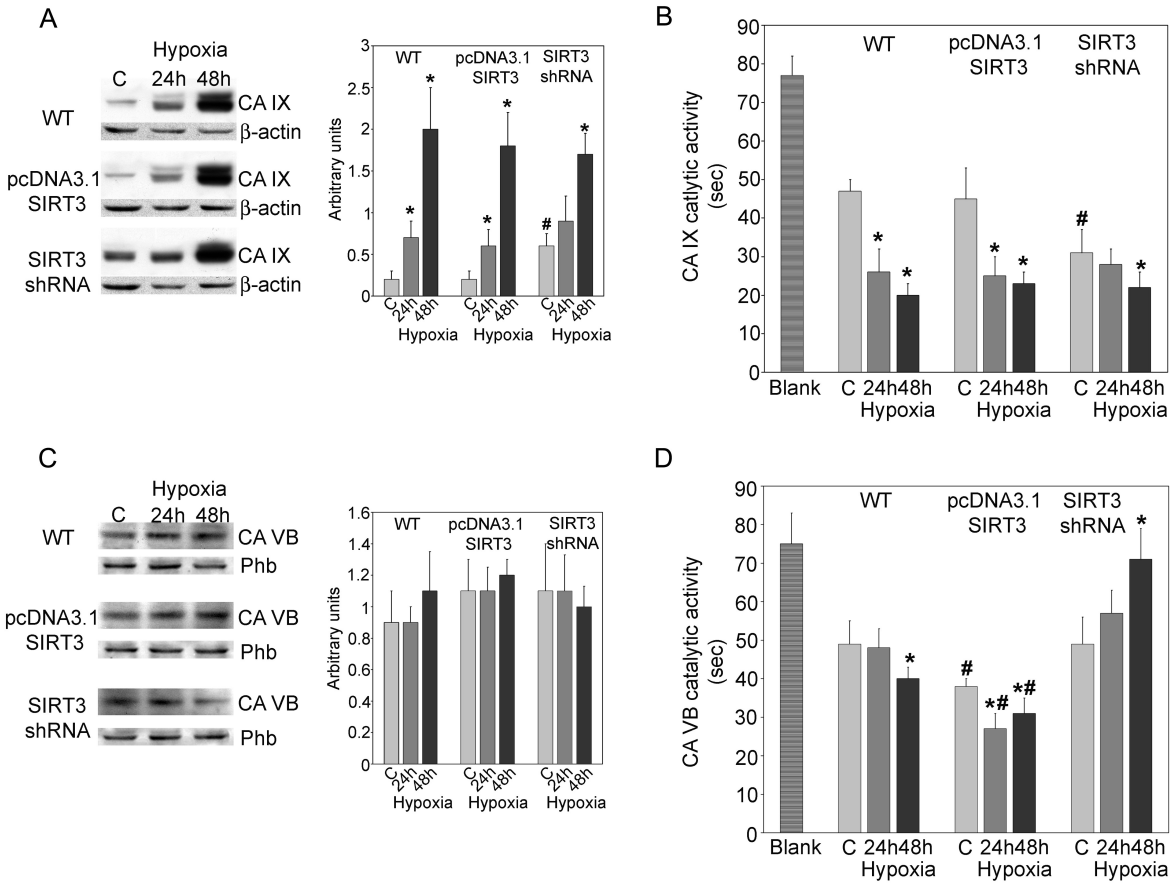

Figure 14. (A) MDA-MB-231 WT, SIRT3-overexpressing and SIRT3-silenced cells were incubated under normoxia or hypoxia for 24 and 48 h. Whole extracts were obtained and CA IX content measured as described under Materials and Methods. Data are representative of at least three separate experiments. b-actin was used as a loading control for total lysate. Histograms on the right side represent average CA IX level relative to b-actin. *Significantly different from C. #Significantly different from control normoxic WT and SIRT3-overexpressing cells. Significance was set at $P<0.05$. **(B)** MDA-MB-231 WT, SIRT3-overexpressing and SIRT3-silenced cells were incubated under normoxia or hypoxia for 24 and 48 h. CA IX catalytic activity, in seconds, was measured in intact cells as described under Materials and Methods. Data are representative of at least three separate experiments. Blank represents chemical reaction without cells. *Significantly different from C. #Significantly different from control normoxic WT and SIRT3-overexpressing cells. Significance was set at $P<0.05$. **(C)** MDA-MB-231 WT, SIRT3-overexpressing and SIRT3-silenced cells were incubated under normoxia or hypoxia for 24 and 48 h. Mitochondrial fractions were obtained and CA VB content measured as described under Materials and Methods. Data are representative of at least three separate experiments. Phb was used as a loading control for mitochondrial lysates. Histograms on the right side represent average CA VB level relative to Phb. **(D)** MDA-MB-231 WT, SIRT3-overexpressing and SIRT3-silenced cells were incubated under normoxia or hypoxia for 24 and 48 h. CA VB catalytic activity, in seconds, was measured in mitochondrial extracts as described under Materials and Methods. Data are representative of at least three separate experiments. Blank represents chemical reaction without cells. *Significantly different from C. #Significantly different from normoxic and hypoxic WT and SIRT3-silenced cells. Significance was set at $P<0.05$

4.4 SIRT3 effects on mitochondrial apoptotic pathway.

SIRT3 controls HKII binding to the PTP that in turn promotes release of proapoptotic factors [96]. On the other hand, SIRT3 controls CA VB activity and consequently pH_i. Intracellular acidification represents a mechanism that causes conformational change and mitochondrial accumulation of the proapoptotic protein Bax [150]. Mitochondrial Bax exacerbates PTP opening with release of apoptogenic factors [150]. Mitochondrial accumulation of Bax in the presence of hypoxia or STS is shown in Figure 15A. In WT and SIRT3-silenced cells, 36h hypoxia exposure resulted in Bax translocation from cytosol to mitochondria. By contrast, SIRT3-overexpressing cells did not show any mitochondrial accumulation of Bax (Figure 15A). Again, STS treatment increased Bax in the mitochondrial fraction of both WT and SIRT3-silenced cells, whereas Bax accumulation was absent in the mitochondria of SIRT3-overexpressing cells (Figure 15A right side). Moreover, whole cellular levels of the anti-apoptotic protein Bcl-2 were significantly increased only in SIRT3-overexpressing cells (Figure 15B).

Induction of MPT, followed by cytochrome c release from mitochondria, is an important step of the apoptotic process [151]. Figure 15C shows that in WT MDA-MB-231 cells hypoxia caused cytochrome c release from mitochondria and accumulation in the cytosol at 72h. SIRT3 overexpression inhibited cytochrome c release, whereas SIRT3 silencing induced a significant loss of cytochrome c from the mitochondria (Figure 15C). Progression of the apoptotic process was documented by the cleavage of the caspase 3 substrate poly(ADP-ribose) polymerase (PARP). After 72 h of hypoxia, PARP was cleaved in WT and SIRT3-silenced cells, whereas no cleavage was observed in SIRT3-overexpressing cells (Figure 15C). Similarly, STS treatment was followed by cytochrome c release and PARP cleavage in WT and in SIRT3-silenced cells. No cytochrome c release and PARP cleavage was observed in SIRT3-overexpressing cells (Figure 15C right side).

Another documented effect of mitochondrial damage and apoptosis is the release of the AIF that accumulates in the nucleus causing DNA degradation [152]. Figure 15D shows AIF nuclear accumulation in WT and SIRT3-silenced cells following hypoxia or STS treatment. By contrast, SIRT3 overexpression completely inhibited nuclear accumulation of AIF (Figure 15D).

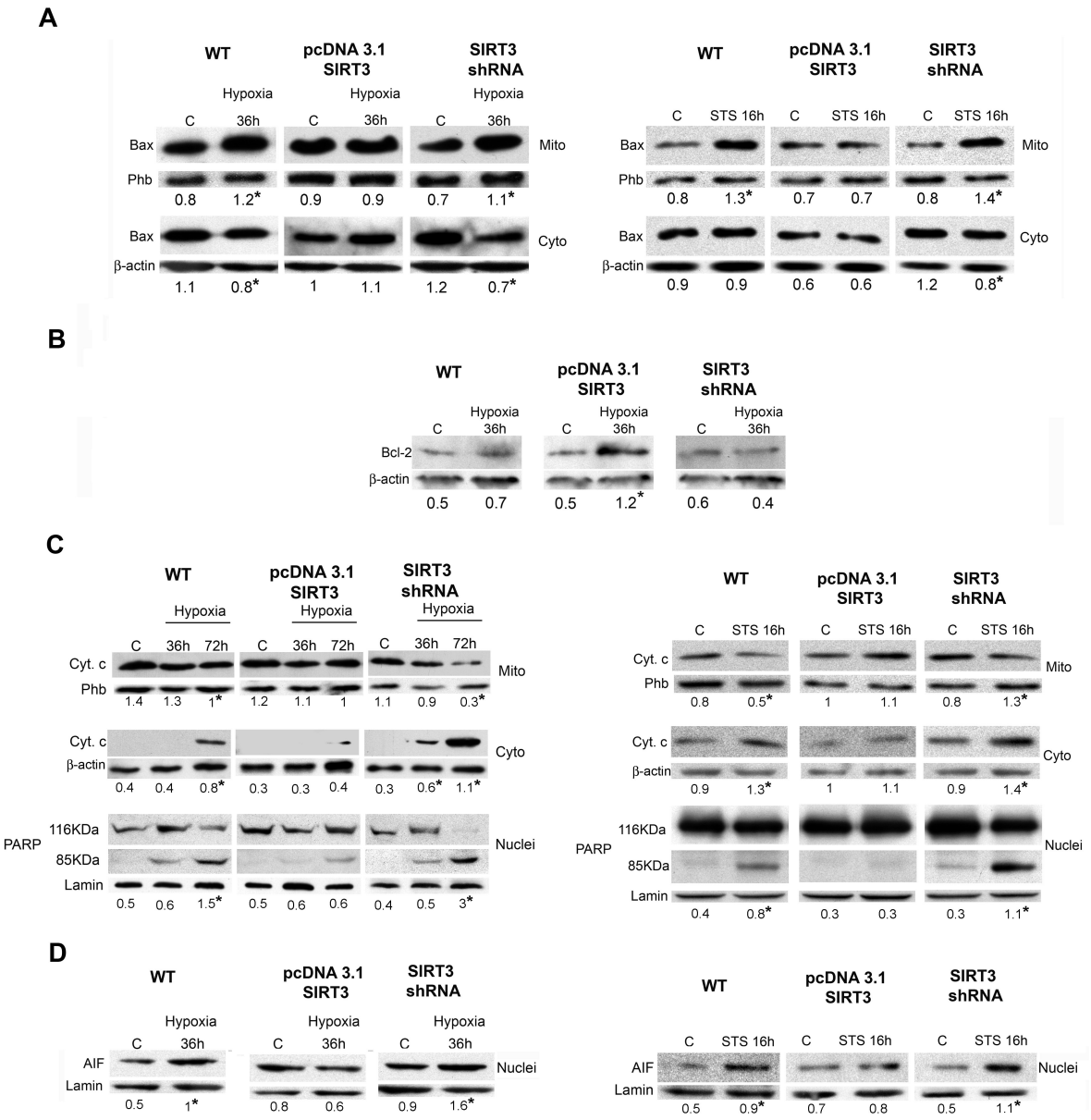

Figure 15. (A) MDA-MB-231 WT, SIRT3-overexpressing and SIRT3-silenced cells were incubated under normoxia or hypoxia for 36 h. Cells were then processed to obtain mitochondrial and cytosolic fractions. Bax levels were assessed by western blot on mitochondria and cytosol as described under Materials and Methods. Data are representative of at least three separate experiments. Phb was used as loading control for mitochondria whereas β-actin was used as a loading control for cytosol. Numbers below each blot represent average level of Bax protein, relative to either Phb or b-actin. *Significantly different from control normoxic cells (C). Significance was set at $P<0.05$. **(B)** MDA-MB-231 WT, SIRT3-overexpressing and SIRT3-silenced cells were incubated under normoxia or hypoxia for 36 h. Cells were then processed to obtain whole-cell lysates. Bcl-2 levels were assessed by western blot as described under Materials and Methods. Data are representative of at least three separate experiments. β-actin was used as a loading control. Numbers below each blot represent average level of Bcl-2 protein, relative to β-actin. *Significantly different from C. Significance was set at $P<0.05$. **(C)** MDA-MB-231 WT, SIRT3-overexpressing and SIRT3-silenced cells were incubated under normoxia, hypoxia or STS for the times indicated. Cells were then processed and nuclear, mitochondrial and cytosolic fractions obtained. Cytochrome c levels were assessed by western blot on mitochondria and cytosol as described under Materials and Methods. PARP cleavage was, instead, measured on nuclei as described under Materials and Methods. Data are representative of at least three separate experiments. Phb was used as loading control for mitochondria whereas β-actin was used as a loading control for cytosol. Lamin was used as nuclear loading control. Numbers below each blot represent average level of the indicated protein, relative to either Phb or β-actin or lamin. *Significantly different from C. Significance was set at $P<0.05$. **(D)** MDA-MB-231 WT, SIRT3-overexpressing and SIRT3-silenced cells

were incubated under normoxia, hypoxia or STS for the times indicated. Cells were then processed and nuclear fractions obtained. Nuclear translocation of AIF was measured on nuclei as described under Materials and Methods. Data are representative of at least three separate experiments. Lamin was used as loading control for nuclei. Numbers below each blot represent average AIF level relative to lamin. *Significantly different from C. Significance was set at P<0.05

4.5 Hypoxia increases SIRT3 expression via SP1

As SIRT3 levels influences cellular metabolism and hypoxia represents a metabolic stress, we investigated changes in SIRT3 levels following hypoxia exposure. In fact, those changes may represent an adaptive cellular response to hypoxia that contributes to cell survival under such a stress. Figure 16 shows that hypoxic incubation of MDA-MB-231 cells increased mitochondrial expression and activity of SIRT3 after 17 and 24h. Hypoxia regulation of SIRT3 expression was confirmed also in HeLa and K562 cell lines. Figure 17A shows that in K562 cells SIRT3 expression and activity increased after 17 h to decrease after 48h. In HeLa cells, SIRT3 expression and activity increased from 17 to 72h (Figure 17B)

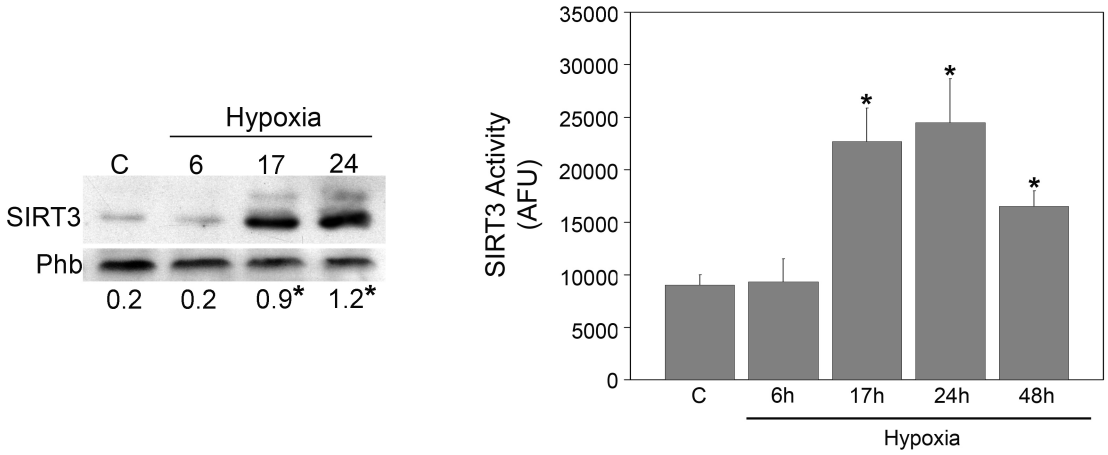

Figure 16. Left side, MDA-MB-231 cells were incubated under normoxic or hypoxic conditions. After the times indicated, cells were processed to obtain a mitochondrial extracts as described under Materials and Methods. The contents of SIRT3 were determined by western blotting. Phb was used as loading control for the mitochondrial fraction. Blots are representative of at least three separate experiments. Numbers below the blots represent average SIRT3 level, relative to Phb. *Significantly different from control normoxic cells (C). Significance was set at P<0.05. Right side, MDA-MB-231 cells were incubated under normoxic or hypoxic conditions. After the times indicated, SIRT3 deacetylase activity was measured on mitochondrial fractions as described under Materials and Methods. Data are representative of at least three separate experiments. Values are represented as mean±S.D. *Significantly different from control normoxic cells. Significance was set at P<0.05

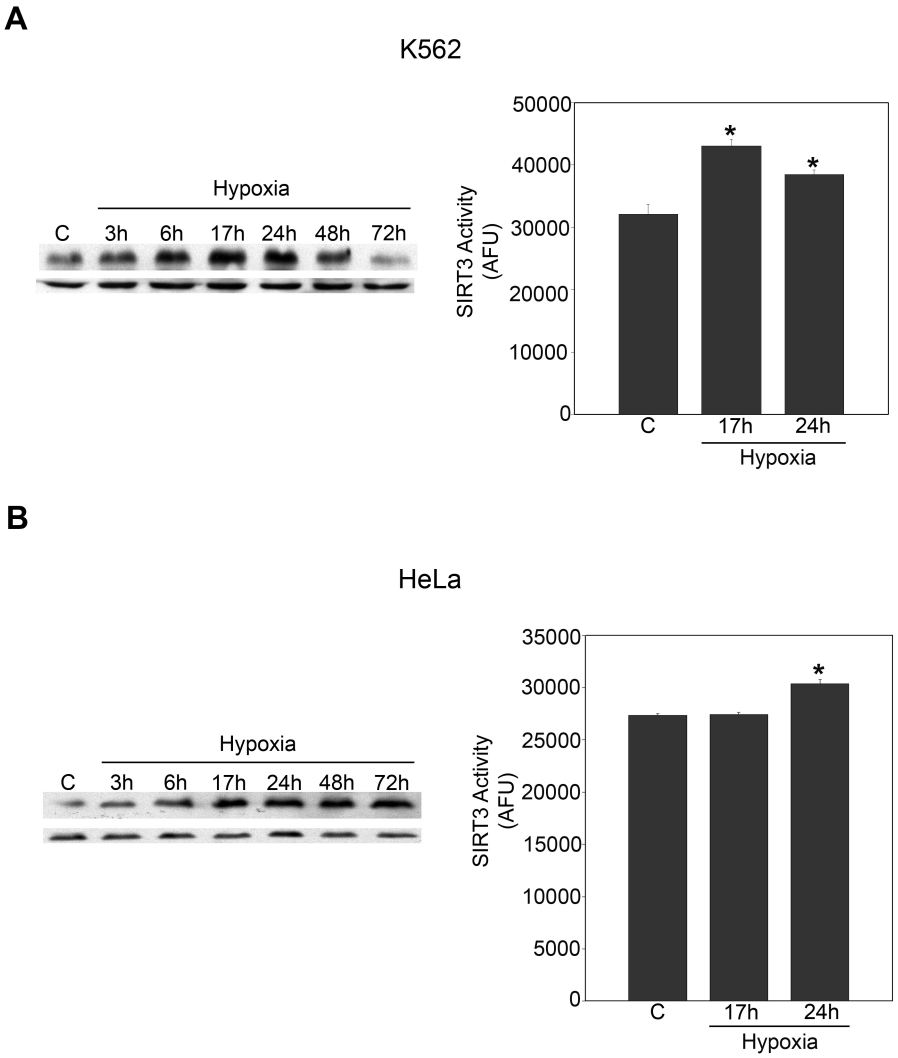

Figure 17. (A) K562 cells were incubated under normoxic or hypoxic conditions. After the times indicated, cells were processed to obtain a whole cell extracts as described under "Materials and Methods". SIRT3 protein levels (left side) and activity (right side) were determined by Western blotting and fluorimetric assay, respectively. b-actin was used as a loading control. Blots are representative of at least three separate experiments. C: control normoxic cells. Values are represented as mean ± s.d. *, significantly different from control normoxic cells. Significance was set at $P<0.05$. **(B)** HeLa cells were incubated under normoxic or hypoxic conditions. After the times indicated, cells were processed to obtain a whole cell extracts as described under "Materials and Methods". SIRT3 protein levels (left side) and activity (right side) were determined by Western blotting and fluorimetric assay, respectively. b-actin was used as a loading control. Blots are representative of at least three separate experiments. C: control normoxic cells. Values are represented as mean ± s.d. *, significantly different from control normoxic cells. Significance was set at $P<0.05$.

In order to evaluate whether SIRT3 increase under hypoxia was mediated by HIF-1α, HIF-1α-silenced cell lines were produced (Figure 18A). Figure 18A (right side) shows that SIRT3 levels were still increased, in HIF-1α-silenced cells, after 4 and 6 h of hypoxia.

SP1 binding sites are clustered in proximity of the SIRT3 transcription start site [153]. Therefore, stable cell lines silenced for SP1 were produced (Figure 18B). Figure 18B (right side) shows that in SP1-silenced cells SIRT3 expression was not detectable under normoxia

and barely detectable under hypoxia (Figure 18B). In order to demonstrate the necessary role of SP1 sites, three constructs were obtained in which luciferase activity is under the control of SIRT3 promoter. In particular, construct A contains all SP1 sites, construct B has none of SP1 sites and construct E is missing three SP1 sites. Figure 18C shows that SP1 sites are important to have a SIRT3 promoter activity and that all SP1 sites are required to have an efficient promoter activity. In fact, we obtained an upregulation in construct A when all SP1 sites were present and a similar downregulation in constructs B and E irrespectively if all or only three SP1 sites were missing (Figure 18C).

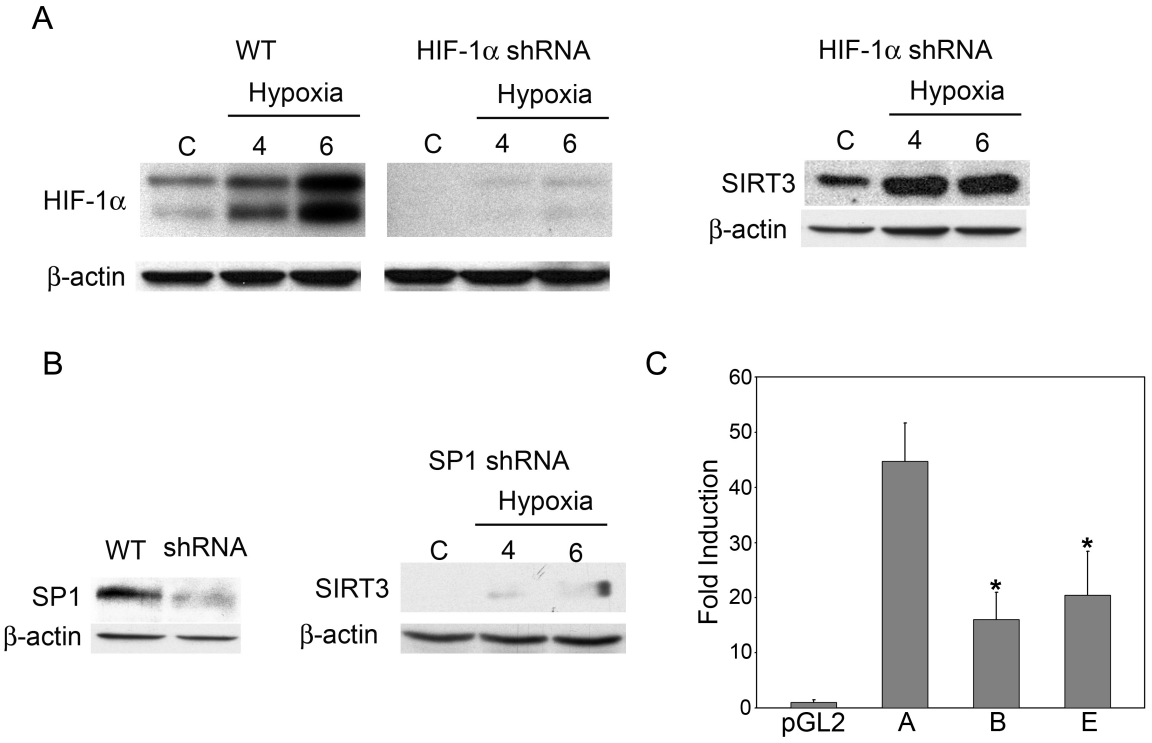

Figure 18. (A) MDA-MB-231 cells either silenced for HIF-1a or transduced with lentiviral empty control particles were incubated under normoxic or hypoxic conditions. After the times indicated, cells were processed to obtain a whole-cell extracts as described under Materials and Methods. The content of HIF-1a (left side) and SIRT3 (right side) were determined by western blotting. β-Actin was used as a whole cells loading control. Blots are representative of at least three separate experiments. C, control normoxic cells. **(B)** MDA-MB-231 either silenced for SP1 or transduced with lentiviral empty control particles were processed to obtain a whole-cell extract as described under Materials and Methods. The content of SP1 was determined by western blotting (left side). SP1-silenced cells were incubated under normoxic or hypoxic conditions for the times indicated. The content of SIRT3 was measured by western blotting (right side). b-Actin was used as a loading control. Blots are representative of at least three separate experiments. C, control normoxic cells. **(C)** Luciferase expression after transient transfection of pGL2 plasmid containing multiple SP1 binding sites of SIRT3 promoter (A), pGL2 plasmid deleted of all the SP1 binding sites of SIRT3 promoter (B) and pGL2 plasmid deleted of three SP1 binding sites of SIRT3 promoter (E) with respect to the pGL2-basic vector. The values reported are the means±S.D. of three independent experiments. *Significantly different from plasmid A. Significance was set at $P<0.05$

5. DISCUSSION

The present study demonstrated that increased expression of SIRT3 protected cells from hypoxia or STS- induced cell death by inhibiting induction of MPT, loss of membrane potential and ROS accumulation. In particular SIRT3 activated CA VB catalytic activity thereby maintaining a physiological pH_i, and inhibited HKII mitochondrial binding thereby decreasing the probability of PTP opening. These two events reduced Bax mitochondrial accumulation and activation of the mitochondrial apoptotic pathway.

In our system we documented that SIRT3 has an important role in protecting hypoxic cells from both apoptosis and necrosis. It is known that tumor cells undergo glycolysis even in the presence of ample oxygen [124]. HKII has a high affinity for glucose and is highly expressed in most tumors localizing on the OMM [154]. Recently, SIRT3 has been shown to induce HKII detachment from OMM by deacetylating cyclophilin D, thereby increasing oxidative phosphorylation [96]. Our results demonstrate that under hypoxia SIRT3 overexpression causes a detachment of HKII from the mitochondria with a decrease in glycolytic rate and a reduction of lactate. Importantly, SIRT3 silencing increased both HKII binding to the mitochondrial fraction and lactate production. HKII increased expression and switch to glycolysis by the tumor cells, accumulates intracellular protons that under 'normal' conditions are decreased by oxidative phosphorylation [155]. Moreover, for the first time, we also show that SIRT3 can regulate pH_i by controlling the activity of the mitochondrial enzyme CA VB. Very little is known about CA VB, however, this enzyme is localized in the mitochondrial matrix and it is ubiquitously expressed [149]. Recently, CA VB has been shown to convert the CO_2 produced by TCA cycle and b-oxidation to HCO_3^- which, in turn controls metabolic pathways increasing oxidative phosphorylation and reducing ROS generation [156]. Moreover, we speculate that the increased CA VB catalytic activity in SIRT3-overexpressing cells, by increasing HCO_3^- production, can buffer protons formed when ATP from cytosolic glycolysis is hydrolyzed by the F1F0 ATPase [157]. The net result of SIRT3 effects on HKII and CA VB is a tight control of pH_i. In fact, a drop in pH_i can activate the proapoptotic protein Bax [158]. Once activated, Bax translocates in the mitochondria inducing the MPT [159]. This sequence of events is reproduced in our model where intracellular acidification followed by mitochondrial accumulation of Bax is more evident in hypoxic SIRT3-silenced cells. By contrast, SIRT3 overexpression prevented intracellular acidification, Bax activation and MPT induction. In fact, only in SIRT3-silenced cells we observed an increase in cytochrome c release, PARP cleavage, nuclear translocation of AIF and cell death. Previously, protection from apoptotic cell death due to

an SIRT3-increased expression has been described in cardiomyocytes where Ku70, a DNA-repair factor and inhibitor of Bax-mediated apoptosis, is deacetylated by SIRT3 hindering the translocation of Bax to mitochondria [101]. Herewith, we propose an alternative or parallel mechanism for SIRT3 protection. SIRT3 by increasing CA VB catalytic activity and by inhibiting HKII mitochondrial binding reduces the glycolytic rate and decreases intracellular acidification. This latter event prevents Bax activation and mitochondrial translocation as well as induction of the MPT.

We also observed that SIRT3 protected cells from necrosis. Our results show that overexpression of SIRT3 reduced LDH as well as HMGB1 release. In particular, HMGB1 is considered a reliable measure of necrosis because it is released only by necrotic cells whereas remains associated to DNA in apoptotic cells [145]. When SIRT3 was silenced ROS, LDH and HMGB1 accumulation were increased both under normoxia and hypoxia.

Interestingly, we also showed that SIRT3 expression increased under hypoxia as part of an adaptive survival mechanism to such metabolic stress that depends by the transcription factor SP1.

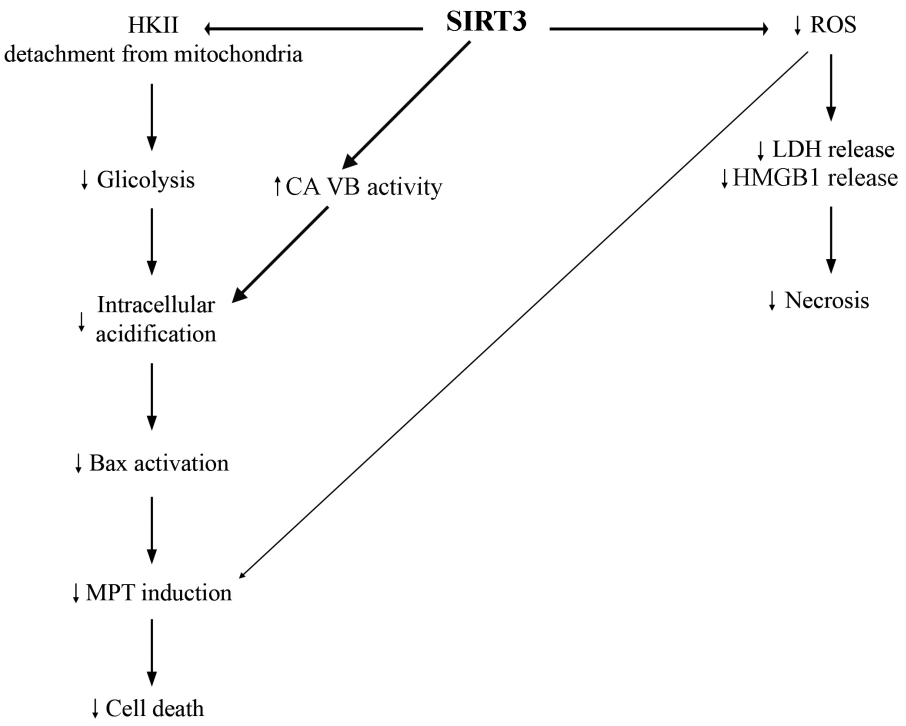

Figure 19. Schematic representation of the pathways controlled by SIRT3. SIRT3 increases cellular resistance to both necrosis and apoptosis by regulating HKII binding to the mitochondria, CA VB catalytic activity and ROS production

On the basis of our results we have drawn a schematic illustration to explain the central role of SIRT3 in mitochondrial cell death (Figure 19). SIRT3 is involved in the reduction of ROS, an event that to one side diminishes LDH and HMGB1 release reducing necrosis, and to the other prevents MPT induction reducing apoptosis. At the same time SIRT3 induces HKII detachment from mitochondrial membrane reducing glycolitic rate and increases catalytic activity of mitochondrial CA VB thereby controlling pH_i. The molecular mechanism through which SIRT3 controls CA VB activity is presently under study. We presume that SIRT3 could deacetylate CA VB, thereby increasing its activity. In fact, SIRT3 and CA VB are both in the mitochondrial matrix and CA VB presents predicted acetylation sites (lysines) as assessed by the online predictor for protein acetylation PAIL, (prediction of acetylation on internal lysines) [160]. In conclusion, by controlling intracellular acidification, SIRT3 reduces Bax activation and mitochondrial translocation inhibiting mitochondrial apoptosis.

6. REFERENCES

1. Klar, A. J., Fogel, S. & Macleod, K. MAR1-a Regulator of the HMa and HMalpha Loci in *Saccharomyces cerevisiae*. *Genetics* **93**, 37–50 (1979).
2. Rine, J. J. & Herskowitz, I. I. Four genes responsible for a position effect on expression from HML and HMR in *Saccharomyces cerevisiae*. *Genetics* **116**, 9–22 (1987).
3. Gottlieb, S. & Esposito, R. E. A new role for a yeast transcriptional silencer gene, SIR2, in regulation of recombination in ribosomal DNA. *Cell* **56**, 771–776 (1989).
4. Aparicio, O. M., Billington, B. L. & Gottschling, D. E. Modifiers of position effect are shared between telomeric and silent mating-type loci in S. cerevisiae. *Cell* **66**, 1279–1287 (1991).
5. Braunstein, M., Rose, A. B., Holmes, S. G., Allis, C. D. & Broach, J. R. Transcriptional silencing in yeast is associated with reduced nucleosome acetylation. *Genes Dev.* **7**, 592–604 (1993).
6. Brachmann, C. B. *et al.* The SIR2 gene family, conserved from bacteria to humans, functions in silencing, cell cycle progression, and chromosome stability. *Genes Dev.* **9**, 2888–2902 (1995).
7. Derbyshire, M. K., Weinstock, K. G. & Strathern, J. N. HST1, a new member of the SIR2 family of genes. *Yeast* **12**, 631–640 (1996).
8. Hirschey, M. D. Old enzymes, new tricks: sirtuins are NAD(+)-dependent de-acylases. *Cell Metab* **14**, 718–719 (2011).
9. Frye, R. A. Phylogenetic classification of prokaryotic and eukaryotic Sir2-like proteins. *Biochem Biophys Res Commun* **273**, 793–798 (2000).
10. Frye, R. A. Characterization of five human cDNAs with homology to the yeast SIR2 gene: Sir2-like proteins (sirtuins) metabolize NAD and may have protein ADP-ribosyltransferase activity. *Biochem Biophys Res Commun* **260**, 273–279 (1999).
11. Avalos, J. L. J. *et al.* Structure of a Sir2 Enzyme Bound to an Acetylated p53 Peptide. *Molecular Cell* **10**, 13–13 (2002).
12. Chang, J.-H. J. *et al.* Structural basis for the NAD-dependent deacetylase mechanism of Sir2. *J Biol Chem* **277**, 34489–34498 (2002).
13. Finnin, M. S., Donigian, J. R. & Pavletich, N. P. Structure of the histone deacetylase SIRT2. *Nat Struct Mol Biol* **8**, 621–625 (2001).
14. Min, J., Landry, J., Sternglanz, R. & Xu, R. M. Crystal structure of a SIR2 homolog-NAD complex. *Cell* **105**, 269–279 (2001).
15. Zhao, K. K., Chai, X. X., Clements, A. A. & Marmorstein, R. R. Structure and autoregulation of the yeast Hst2 homolog of Sir2. *Nat Struct Mol Biol* **10**, 864–871 (2003).
16. Zhao, K., Chai, X. & Marmorstein, R. Structure of the Yeast Hst2 Protein Deacetylase in Ternary Complex with 2'-O-Acetyl ADP Ribose and Histone Peptide. *Structure* **11**, 1403–1411 (2003).
17. Schwer, B. B., North, B. J. B., Frye, R. A. R., Ott, M. M. & Verdin, E. E. The human silent information regulator (Sir)2 homologue hSIRT3 is a mitochondrial nicotinamide adenine dinucleotide-dependent deacetylase. *J Cell Biol* **158**, 647–657 (2002).
18. Tennen, R. I., Berber, E. & Chua, K. F. Functional dissection of SIRT6: identification of domains that regulate histone deacetylase activity and chromatin localization. *Mech. Ageing Dev.* **131**, 185–192 (2010).
19. Sanders, B. D., Jackson, B. & Marmorstein, R. Structural basis for sirtuin function: what we know and what we don't. *Biochim Biophys Acta* **1804**, 1604–1616 (2010).

20. Rossmann, M. G. & Argos, P. The taxonomy of binding sites in proteins. *Mol Cell Biochem* **21**, 161–182 (1978).
21. Landry, J. *et al.* The silencing protein SIR2 and its homologs are NAD-dependent protein deacetylases. *Proc Natl Acad Sci USA* **97**, 5807–5811 (2000).
22. Smith, J. S. *et al.* A phylogenetically conserved NAD+-dependent protein deacetylase activity in the Sir2 protein family. *Proc Natl Acad Sci USA* **97**, 6658–6663 (2000).
23. Tanner, K. G., Landry, J., Sternglanz, R. & Denu, J. M. Silent information regulator 2 family of NAD-dependent histone/protein deacetylases generates a unique product, 1-O-acetyl-ADP-ribose. *Proc Natl Acad Sci USA* **97**, 14178–14182 (2000).
24. Tanny, J. C. & Moazed, D. Coupling of histone deacetylation to NAD breakdown by the yeast silencing protein Sir2: Evidence for acetyl transfer from substrate to an NAD breakdown product. *Proc Natl Acad Sci USA* **98**, 415–420 (2001).
25. Imai, S., Armstrong, C. M., Kaeberlein, M. & Guarente, L. Transcriptional silencing and longevity protein Sir2 is an NAD-dependent histone deacetylase. *Nature* **403**, 795–800 (2000).
26. Jackson, M. D. & Denu, J. M. Structural identification of 2‘- and 3’-O-acetyl-ADP-ribose as novel metabolites derived from the Sir2 family of beta -NAD+-dependent histone/protein deacetylases. *J Biol Chem* **277**, 18535–18544 (2002).
27. Sauve, A. A. *et al.* Chemistry of gene silencing: the mechanism of NAD+-dependent deacetylation reactions. *Biochemistry* **40**, 15456–15463 (2001).
28. Sauve, A. A., Wolberger, C., Schramm, V. L. & Boeke, J. D. The biochemistry of sirtuins. *Annu. Rev. Biochem.* **75**, 435–465 (2006).
29. Borra, M. T., Langer, M. R., Slama, J. T. & Denu, J. M. Substrate Specificity and Kinetic Mechanism of the Sir2 Family of NAD +-Dependent Histone/Protein Deacetylases †. *Biochemistry* **43**, 9877–9887 (2004).
30. Schmidt, M. T. Coenzyme Specificity of Sir2 Protein Deacetylases: IMPLICATIONS FOR PHYSIOLOGICAL REGULATION. *J Biol Chem* **279**, 40122–40129 (2004).
31. Smith, B. C., Hallows, W. C. & Denu, J. M. Mechanisms and molecular probes of sirtuins. *Chem. Biol.* **15**, 1002–1013 (2008).
32. Sauve, A. A. Pharmaceutical strategies for activating sirtuins. *Curr. Pharm. Des.* **15**, 45–56 (2009).
33. Sauve, A. A. Sirtuin chemical mechanisms. *Biochim Biophys Acta* **1804**, 1591–1603 (2010).
34. Tanny, J. C., Dowd, G. J., Huang, J., Hilz, H. & Moazed, D. An enzymatic activity in the yeast Sir2 protein that is essential for gene silencing. *Cell* **99**, 735–745 (1999).
35. García-Salcedo, J. A., Gijón, P., Nolan, D. P., Tebabi, P. & Pays, E. A chromosomal SIR2 homologue with both histone NAD-dependent ADP-ribosyltransferase and deacetylase activities is involved in DNA repair in Trypanosoma brucei. *EMBO J.* **22**, 5851–5862 (2003).
36. Liszt, G., Ford, E., Kurtev, M. & Guarente, L. Mouse Sir2 homolog SIRT6 is a nuclear ADP-ribosyltransferase. *J Biol Chem* **280**, 21313–21320 (2005).
37. French, J. B., Cen, Y. & Sauve, A. A. Plasmodium falciparum Sir2 is an NAD+-dependent deacetylase and an acetyllysine-dependent and acetyllysine-independent NAD+ glycohydrolase. *Biochemistry* **47**, 10227–10239 (2008).
38. Denu, J. M. The Sir 2 family of protein deacetylases. *Curr Opin Chem Biol* **9**, 431–440 (2005).
39. Du, J. J. *et al.* Sirt5 is a NAD-dependent protein lysine demalonylase and desuccinylase. *Science* **334**, 806–809 (2011).

40. Peng, C. *et al.* The first identification of lysine malonylation substrates and its regulatory enzyme. *Mol. Cell Proteomics* **10**, M111.012658 (2011).
41. Smith, B. C. & Denu, J. M. Acetyl-lysine analog peptides as mechanistic probes of protein deacetylases. *J Biol Chem* **282**, 37256–37265 (2007).
42. Garrity, J., Gardner, J. G., Hawse, W., Wolberger, C. & Escalante-Semerena, J. C. N-lysine propionylation controls the activity of propionyl-CoA synthetase. *J Biol Chem* **282**, 30239–30245 (2007).
43. Bitterman, K. J. K., Anderson, R. M. R., Cohen, H. Y. H., Latorre-Esteves, M. M. & Sinclair, D. A. D. Inhibition of silencing and accelerated aging by nicotinamide, a putative negative regulator of yeast sir2 and human SIRT1. *J Biol Chem* **277**, 45099–45107 (2002).
44. Lin, S.-J. S., Ford, E. E., Haigis, M. M., Liszt, G. G. & Guarente, L. L. Calorie restriction extends yeast life span by lowering the level of NADH. *Genes Dev.* **18**, 12–16 (2004).
45. Shore, D., Squire, M. & Nasmyth, K. A. Characterization of two genes required for the position-effect control of yeast mating-type genes. *EMBO J.* **3**, 2817 (1984).
46. Zhong, L. *et al.* The histone deacetylase Sirt6 regulates glucose homeostasis via Hif1alpha. *Cell* **140**, 280–293 (2010).
47. Shi, T., Wang, F., Stieren, E. & Tong, Q. SIRT3, a mitochondrial sirtuin deacetylase, regulates mitochondrial function and thermogenesis in brown adipocytes. *J Biol Chem* **280**, 13560–13567 (2005).
48. Michishita, E. *et al.* SIRT6 is a histone H3 lysine 9 deacetylase that modulates telomeric chromatin. *Nature* **452**, 492–496 (2008).
49. Nakagawa, T., Lomb, D. J., Haigis, M. C. & Guarente, L. SIRT5 Deacetylates Carbamoyl Phosphate Synthetase 1 and Regulates the Urea Cycle. *Cell* **137**, 560–570 (2009).
50. Michishita, E., Park, J. Y., Burneskis, J. M., Barrett, J. C. & Horikawa, I. Evolutionarily conserved and nonconserved cellular localizations and functions of human SIRT proteins. *Mol Biol Cell* **16**, 4623–4635 (2005).
51. Tanno, M., Sakamoto, J., Miura, T., Shimamoto, K. & Horio, Y. Nucleocytoplasmic shuttling of the NAD+-dependent histone deacetylase SIRT1. *J Biol Chem* **282**, 6823–6832 (2007).
52. North, B. J., Marshall, B. L., Borra, M. T., Denu, J. M. & Verdin, E. The Human Sir2 Ortholog, SIRT2, Is an NAD+-Dependent Tubulin Deacetylase. *Molecular Cell* **11**, 437–444 (2003).
53. Jing, E., Gesta, S. & Kahn, C. R. SIRT2 Regulates Adipocyte Differentiation through FoxO1 Acetylation/Deacetylation. *Cell Metab* **6**, 10–10 (2007).
54. Dryden, S. C. S., Nahhas, F. A. F., Nowak, J. E. J., Goustin, A.-S. A. & Tainsky, M. A. M. Role for human SIRT2 NAD-dependent deacetylase activity in control of mitotic exit in the cell cycle. *Molecular and Cellular Biology* **23**, 3173–3185 (2003).
55. Vaquero, A. A. *et al.* SirT2 is a histone deacetylase with preference for histone H4 Lys 16 during mitosis. *Genes Dev.* **20**, 1256–1261 (2006).
56. Lampson, M. A. & Kapoor, T. M. The human mitotic checkpoint protein BubR1 regulates chromosome-spindle attachments. *Nat. Cell Biol.* **7**, 93–98 (2005).
57. Jiang, W. *et al.* Acetylation Regulates Gluconeogenesis by Promoting PEPCK1 Degradation via Recruiting the UBR5 Ubiquitin Ligase. *Molecular Cell* **43**, 12–12 (2011).
58. Rothgiesser, K. M., Erener, S., Waibel, S., Luscher, B. & Hottiger, M. O. SIRT2 regulates NF-κB dependent gene expression through deacetylation of p65 Lys310. *Journal of Cell Science* **123**, 4251–4258 (2010).
59. Black, J. C. J., Mosley, A. A., Kitada, T. T., Washburn, M. M. & Carey, M. M.

The SIRT2 Deacetylase Regulates Autoacetylation of p300. *Molecular Cell* **32**, 449–455 (2008).
60. Narayan, N. *et al.* The NAD-dependent deacetylase SIRT2 is required for programmed necrosis. *Nature* **492**, 199–204 (2012).
61. Mostoslavsky, R. *et al.* Genomic Instability and Aging-like Phenotype in the Absence of Mammalian SIRT6. *Cell* **124**, 315–329 (2006).
62. Michishita, E. E. *et al.* Cell cycle-dependent deacetylation of telomeric histone H3 lysine K56 by human SIRT6. *Cell Cycle* **8**, 2664–2666 (2009).
63. Yang, B., Zwaans, B. M. M., Eckersdorff, M. & Lombard, D. B. The sirtuin SIRT6 deacetylates H3 K56Ac in vivo to promote genomic stability. *Cell Cycle* **8**, 2662–2663 (2009).
64. Mao, Z. Z. *et al.* SIRT6 promotes DNA repair under stress by activating PARP1. *Science* **332**, 1443–1446 (2011).
65. Jia, G. G., Su, L. L., Singhal, S. S. & Liu, X. X. Emerging roles of SIRT6 on telomere maintenance, DNA repair, metabolism and mammalian aging. *Mol Cell Biochem* **364**, 345–350 (2012).
66. Kawahara, T. L. A. *et al.* SIRT6 links histone H3 lysine 9 deacetylation to NF-kappaB-dependent gene expression and organismal life span. *Cell* **136**, 62–74 (2009).
67. Xiao, C. *et al.* Progression of Chronic Liver Inflammation and Fibrosis Driven by Activation of c-JUN Signaling in Sirt6 Mutant Mice. *Journal of Biological Chemistry* **287**, 41903–41913 (2012).
68. Ford, E. *et al.* Mammalian Sir2 homolog SIRT7 is an activator of RNA polymerase I transcription. *Genes Dev.* **20**, 1075–1080 (2006).
69. Grob, A. *et al.* Involvement of SIRT7 in resumption of rDNA transcription at the exit from mitosis. *Journal of Cell Science* **122**, 489–498 (2009).
70. Barber, M. F. *et al.* SIRT7 links H3K18 deacetylation to maintenance of oncogenic transformation. *Nature* **487**, 114–118 (2012).
71. Vakhrusheva, O. *et al.* Sirt7 increases stress resistance of cardiomyocytes and prevents apoptosis and inflammatory cardiomyopathy in mice. *Circ. Res.* **102**, 703–710 (2008).
72. PhD, E. P., Sasso PhD, Lo, G. & PhD, J. A. M. Mitochondrial sirtuins and metabolic homeostasis. *Best Pract. Res. Clin. Endocrinol. Metab.* **26**, 759–770 (2012).
73. Haigis, M. C. *et al.* SIRT4 inhibits glutamate dehydrogenase and opposes the effects of calorie restriction in pancreatic beta cells. *Cell* **126**, 941–954 (2006).
74. Verdin, E., Hirschey, M. D., Finley, L. W. S. & Haigis, M. C. Sirtuin regulation of mitochondria: energy production, apoptosis, and signaling. *Trends in Biochemical Sciences* **35**, 669–675 (2010).
75. Ahuja, N. *et al.* Regulation of insulin secretion by SIRT4, a mitochondrial ADP-ribosyltransferase. *J Biol Chem* **282**, 33583–33592 (2007).
76. Verma, M., Shulga, N. & Pastorino, J. G. Sirtuin-4 modulates sensitivity to induction of the mitochondrial permeability transition pore. *Biochim Biophys Acta* (2012).doi:10.1016/j.bbabio.2012.09.016
77. Onyango, P., Celic, I., McCaffery, J. M., Boeke, J. D. & Feinberg, A. P. SIRT3, a human SIR2 homologue, is an NAD-dependent deacetylase localized to mitochondria. *Proc Natl Acad Sci USA* **99**, 13653–13658 (2002).
78. Lombard, D. B. *et al.* Mammalian Sir2 homolog SIRT3 regulates global mitochondrial lysine acetylation. *Molecular and Cellular Biology* **27**, 8807–8814 (2007).
79. Sol, E. M. *et al.* Proteomic investigations of lysine acetylation identify diverse substrates of mitochondrial deacetylase sirt3. *PLoS ONE* **7**, e50545 (2012).

80. Scher, M. B., Vaquero, A. & Reinberg, D. SirT3 is a nuclear NAD+-dependent histone deacetylase that translocates to the mitochondria upon cellular stress. *Genes Dev.* **21**, 920–928 (2007).
81. Nakamura, Y., Ogura, M., Tanaka, D. & Inagaki, N. Localization of mouse mitochondrial SIRT proteins: Shift of SIRT3 to nucleus by co-expression with SIRT5. *Biochem Biophys Res Commun* **366**, 174–179 (2008).
82. Hallows, W. C., Albaugh, B. N. & Denu, J. M. Where in the cell is SIRT3?--functional localization of an NAD+-dependent protein deacetylase. *Biochem J* **411**, e11–3 (2008).
83. Sundaresan, N. R. *et al.* Sirt3 blocks the cardiac hypertrophic response by augmenting Foxo3a-dependent antioxidant defense mechanisms in mice. *J. Clin. Invest.* **119**, 2758–2771 (2009).
84. Iwahara, T., Bonasio, R., Narendra, V. & Reinberg, D. SIRT3 Functions in the Nucleus in the Control of Stress-Related Gene Expression. *Molecular and Cellular Biology* (2012).doi:10.1128/MCB.00822-12
85. Finley, L. W. S. & Haigis, M. C. Metabolic regulation by SIRT3: implications for tumorigenesis. *Trends Mol Med* **18**, 516–523 (2012).
86. Ahn, B.-H. *et al.* A role for the mitochondrial deacetylase Sirt3 in regulating energy homeostasis. *Proc Natl Acad Sci USA* **105**, 14447–14452 (2008).
87. Finley, L. W. S. *et al.* Succinate dehydrogenase is a direct target of sirtuin 3 deacetylase activity. *PLoS ONE* **6**, e23295 (2011).
88. Cimen, H. *et al.* Regulation of Succinate Dehydrogenase Activity by SIRT3 in Mammalian Mitochondria. *Biochemistry* **49**, 304–311 (2010).
89. Jing, E. *et al.* Sirtuin-3 (Sirt3) regulates skeletal muscle metabolism and insulin signaling via altered mitochondrial oxidation and reactive oxygen species production. *Proc Natl Acad Sci USA* **108**, 14608–14613 (2011).
90. Hirschey, M. D. M. *et al.* SIRT3 regulates mitochondrial fatty-acid oxidation by reversible enzyme deacetylation. *Nature* **464**, 121–125 (2010).
91. Schlicker, C. *et al.* Substrates and regulation mechanisms for the human mitochondrial sirtuins Sirt3 and Sirt5. *Journal of Molecular Biology* **382**, 790–801 (2008).
92. Shimazu, T. T. *et al.* SIRT3 Deacetylates Mitochondrial 3-Hydroxy-3-Methylglutaryl CoA Synthase 2 and Regulates Ketone Body Production. *Cell Metab* **12**, 8–8 (2010).
93. Hallows, W. C. Sirtuins deacetylate and activate mammalian acetyl-CoA synthetases. *Proc Natl Acad Sci USA* **103**, 10230–10235 (2006).
94. Schwer, B., Bunkenborg, J., Verdin, R. O., Andersen, J. S. & Verdin, E. Reversible lysine acetylation controls the activity of the mitochondrial enzyme acetyl-CoA synthetase 2. *Proc Natl Acad Sci USA* **103**, 10224–10229 (2006).
95. Hallows, W. C. *et al.* Sirt3 promotes the urea cycle and fatty acid oxidation during dietary restriction. *Molecular Cell* **41**, 139–149 (2011).
96. Shulga, N., Wilson-Smith, R. & Pastorino, J. G. Sirtuin-3 deacetylation of cyclophilin D induces dissociation of hexokinase II from the mitochondria. *Journal of Cell Science* **123**, 894–902 (2010).
97. Giorgio, V. *et al.* Cyclophilin D in mitochondrial pathophysiology. *Biochim Biophys Acta* **1797**, 1113–1118 (2010).
98. Shulga, N. & Pastorino, J. G. Ethanol sensitizes mitochondria to the permeability transition by inhibiting deacetylation of cyclophilin-D mediated by sirtuin-3. *Journal of Cell Science* **123**, 4117–4127 (2010).
99. Li, Y., Johnson, N., Capano, M., Edwards, M. & CROMPTON, M. Cyclophilin-D promotes the mitochondrial permeability transition but has opposite effects on apoptosis and necrosis. *Biochem J* **383**, 101–109 (2004).

100. Schubert, A. & Grimm, S. Cyclophilin D, a component of the permeability transition-pore, is an apoptosis repressor. *Cancer Research* **64**, 85–93 (2004).
101. Sundaresan, N. R., Samant, S. A., Pillai, V. B., Rajamohan, S. B. & Gupta, M. P. SIRT3 is a stress-responsive deacetylase in cardiomyocytes that protects cells from stress-mediated cell death by deacetylation of Ku70. *Molecular and Cellular Biology* **28**, 6384–6401 (2008).
102. Qiu, X., Brown, K., Hirschey, M. D., Verdin, E. & Chen, D. Calorie restriction reduces oxidative stress by SIRT3-mediated SOD2 activation. *Cell Metab* **12**, 662–667 (2010).
103. Tao, R. *et al.* Sirt3-mediated deacetylation of evolutionarily conserved lysine 122 regulates MnSOD activity in response to stress. *Molecular Cell* **40**, 893–904 (2010).
104. Someya, S. *et al.* Sirt3 mediates reduction of oxidative damage and prevention of age-related hearing loss under caloric restriction. *Cell* **143**, 802–812 (2010).
105. Jacobs, K. M. *et al.* SIRT3 interacts with the daf-16 homolog FOXO3a in the mitochondria, as well as increases FOXO3a dependent gene expression. *Int. J. Biol. Sci.* **4**, 291–299 (2008).
106. Hafner, A. V. *et al.* Regulation of the mPTP by SIRT3-mediated deacetylation of CypD at lysine 166 suppresses age-related cardiac hypertrophy. *Aging (Albany NY)* **2**, 914–923 (2010).
107. Kim, H.-S. *et al.* SIRT3 is a mitochondria-localized tumor suppressor required for maintenance of mitochondrial integrity and metabolism during stress. *Cancer Cell* **17**, 41–52 (2010).
108. Finley, L. W. S. *et al.* SIRT3 Opposes Reprogramming of Cancer Cell Metabolism through HIF1α Destabilization. *Cancer Cell* **19**, 416–428 (2011).
109. Alhazzazi, T. Y., Kamarajan, P., Verdin, E. & Kapila, Y. L. SIRT3 and cancer: tumor promoter or suppressor? *Biochim Biophys Acta* **1816**, 80–88 (2011).
110. Ashraf, N. *et al.* Altered sirtuin expression is associated with node-positive breast cancer. *Br. J. Cancer* **95**, 1056–1061 (2006).
111. Zhang, Y.-Y. & Zhou, L.-M. Sirt3 inhibits hepatocellular carcinoma cell growth through reducing Mdm2-mediated p53 degradation. *Biochem Biophys Res Commun* **423**, 26–31 (2012).
112. Kamarajan, P. *et al.* Receptor-interacting protein (RIP) and Sirtuin-3 (SIRT3) are on opposite sides of anoikis and tumorigenesis. *Cancer* **118**, 5800–5810 (2012).
113. GRAY, L. H., CONGER, A. D., EBERT, M., HORNSEY, S. & SCOTT, O. C. The concentration of oxygen dissolved in tissues at the time of irradiation as a factor in radiotherapy. *Br J Radiol* **26**, 638–648 (1953).
114. THOMLINSON, R. H. & GRAY, L. H. The histological structure of some human lung cancers and the possible implications for radiotherapy. *Br. J. Cancer* **9**, 539–549 (1955).
115. O'Reilly, M. S., Holmgren, L., Chen, C. & Folkman, J. Angiostatin induces and sustains dormancy of human primary tumors in mice. *Nat. Med.* **2**, 689–692 (1996).
116. Wang, G. L., Jiang, B. H., Rue, E. A. & Semenza, G. L. Hypoxia-inducible factor 1 is a basic-helix-loop-helix-PAS heterodimer regulated by cellular O2 tension. *Proc Natl Acad Sci USA* **92**, 5510–5514 (1995).
117. Wang, G. L. & Semenza, G. L. Purification and characterization of hypoxia-inducible factor 1. *J Biol Chem* **270**, 1230–1237 (1995).
118. Maxwell, P. H. *et al.* The tumour suppressor protein VHL targets hypoxia-inducible factors for oxygen-dependent proteolysis. *Nature* **399**, 271–275 (1999).
119. Huang, L. E., Arany, Z., Livingston, D. M. & Bunn, H. F. Activation of hypoxia-inducible transcription factor depends primarily upon redox-sensitive stabilization

of its alpha subunit. *J Biol Chem* **271**, 32253–32259 (1996).
120. Kallio, P. J., Pongratz, I., Gradin, K., McGuire, J. & Poellinger, L. Activation of hypoxia-inducible factor 1alpha: posttranscriptional regulation and conformational change by recruitment of the Arnt transcription factor. *Proc Natl Acad Sci USA* **94**, 5667–5672 (1997).
121. Wenger, R. H., Stiehl, D. P. & Camenisch, G. Integration of oxygen signaling at the consensus HRE. *Sci. STKE* **2005**, re12 (2005).
122. Semenza, G. L. Defining the role of hypoxia-inducible factor 1 in cancer biology and therapeutics. *Oncogene* **29**, 625–634 (2010).
123. Bell, E. L., Emerling, B. M., Ricoult, S. J. H. & Guarente, L. SirT3 suppresses hypoxia inducible factor 1α and tumor growth by inhibiting mitochondrial ROS production. *Oncogene* 1–11 (2011).
124. WARBURG, O. On the origin of cancer cells. *Science* **123**, 309–314 (1956).
125. Tong, X., Zhao, F. & Thompson, C. B. The molecular determinants of de novo nucleotide biosynthesis in cancer cells. *Curr. Opin. Genet. Dev.* **19**, 32–37 (2009).
126. Gatenby, R. A. & Gillies, R. J. Why do cancers have high aerobic glycolysis? *Nat. Rev. Cancer* **4**, 891–899 (2004).
127. Lim, J.-H. *et al.* Sirtuin 1 modulates cellular responses to hypoxia by deacetylating hypoxia-inducible factor 1alpha. *Molecular Cell* **38**, 864–878 (2010).
128. Dioum, E. M. *et al.* Regulation of hypoxia-inducible factor 2alpha signaling by the stress-responsive deacetylase sirtuin 1. *Science* **324**, 1289–1293 (2009).
129. Chen, R., Dioum, E. M., Hogg, R. T., Gerard, R. D. & Garcia, J. A. Hypoxia increases sirtuin 1 expression in a hypoxia-inducible factor-dependent manner. *Journal of Biological Chemistry* **286**, 13869–13878 (2011).
130. Galluzzi, L. *et al.* Molecular definitions of cell death subroutines: recommendations of the Nomenclature Committee on Cell Death 2012. *Cell Death Differ.* **19**, 107–120 (2012).
131. Kerr, J. F. J., Wyllie, A. H. A. & Currie, A. R. A. Apoptosis: a basic biological phenomenon with wide-ranging implications in tissue kinetics. *Br. J. Cancer* **26**, 239–257 (1972).
132. Martin, S. J. & Green, D. R. Protease activation during apoptosis: death by a thousand cuts? *Cell* **82**, 349–352 (1995).
133. Cohen, G. M. *et al.* Formation of large molecular weight fragments of DNA is a key committed step of apoptosis in thymocytes. *J. Immunol.* **153**, 507–516 (1994).
134. Golstein, P. & Kroemer, G. Cell death by necrosis: towards a molecular definition. *Trends in Biochemical Sciences* **32**, 37–43 (2007).
135. Festjens, N., Vanden Berghe, T. & Vandenabeele, P. Necrosis, a well-orchestrated form of cell demise: signalling cascades, important mediators and concomitant immune response. *Biochim Biophys Acta* **1757**, 1371–1387 (2006).
136. Kinnally, K. W., Peixoto, P. M., Ryu, S.-Y. & Dejean, L. M. Is mPTP the gatekeeper for necrosis, apoptosis, or both? *Biochim Biophys Acta* **1813**, 616–622 (2011).
137. Halestrap, A. P. What is the mitochondrial permeability transition pore? *Journal of Molecular and Cellular Cardiology* **46**, 821–831 (2009).
138. Baines, C. P. C. *et al.* Loss of cyclophilin D reveals a critical role for mitochondrial permeability transition in cell death. *Nature* **434**, 658–662 (2005).
139. Nakagawa, T. T. *et al.* Cyclophilin D-dependent mitochondrial permeability transition regulates some necrotic but not apoptotic cell death. *Nature* **434**, 652–658 (2005).
140. Schinzel, A. C. A. *et al.* Cyclophilin D is a component of mitochondrial permeability transition and mediates neuronal cell death after focal cerebral ischemia. *Proc Natl Acad Sci USA* **102**, 12005–12010 (2005).

141. De Giorgi, F. F. *et al.* The permeability transition pore signals apoptosis by directing Bax translocation and multimerization. *FASEB J.* **16**, 607–609 (2002).
142. Scorrano, L. & Korsmeyer, S. J. Mechanisms of cytochrome c release by proapoptotic BCL-2 family members. *Biochemical and biophysical research ...* (2003).
143. Honda, H. M. & Ping, P. Mitochondrial Permeability Transition in Cardiac Cell Injury and Death. *Cardiovasc Drugs Ther* **20**, 425–432 (2006).
144. Nilsson, C., Kågedal, K., Johansson, U. & Ollinger, K. Analysis of cytosolic and lysosomal pH in apoptotic cells by flow cytometry. *Methods Cell Sci* **25**, 185–194 (2003).
145. Krysko, D. V., Berghe, T. V., Parthoens, E., D'Herde, K. & Vandenabeele, P. Chapter 16 Methods for Distinguishing Apoptotic from Necrotic Cells and Measuring Their Clearance. *Methods Enzymol* **442**, 35–35 (2007).
146. Mathupala, S. P., Ko, Y. H. & Pedersen, P. L. Hexokinase II: cancer's double-edged sword acting as both facilitator and gatekeeper of malignancy when bound to mitochondria. *Oncogene* **25**, 4777–4786 (2006).
147. Susin, S. A., Zamzami, N. & Kroemer, G. Mitochondria as regulators of apoptosis: doubt no more. *Biochim Biophys Acta* **1366**, 151–165 (1998).
148. Madshus, I. H. Regulation of intracellular pH in eukaryotic cells. *Biochemical Journal* (1988).
149. Gilmour, K. M. Perspectives on carbonic anhydrase. *Comparative Biochemistry and Physiology Part A: Molecular & Integrative Physiology* **157**, 193–197 (2010).
150. Tafani, M. *et al.* Regulation of intracellular pH mediates Bax activation in HeLa cells treated with staurosporine or tumor necrosis factor-alpha. *THE JOURNAL OF BIOLOGICAL CHEMISTRY* **277**, 49569–49576 (2002).
151. Liu, X., Kim, C. N., Yang, J., Jemmerson, R. & Wang, X. Induction of apoptotic program in cell-free extracts: requirement for dATP and cytochrome c. *Cell* **86**, 147–157 (1996).
152. Penninger, J. M. & Kroemer, G. Mitochondria, AIF and caspases--rivaling for cell death execution. *Nat. Cell Biol.* **5**, 97–99 (2003).
153. Bellizzi, D. *et al.* Characterization of a bidirectional promoter shared between two human genes related to aging: SIRT3 and PSMD13. *Genomics* **89**, 143–150 (2007).
154. Mathupala, S. P., Rempel, A. & Pedersen, P. L. Glucose catabolism in cancer cells: identification and characterization of a marked activation response of the type II hexokinase gene to hypoxic conditions. *J Biol Chem* **276**, 43407–43412 (2001).
155. VAGHY, P. Role of mitochondrial oxidative phosphorylation in the maintenance of intracellular pH*1. *Journal of Molecular and Cellular Cardiology* **11**, 933–940 (1979).
156. Acin-Perez, R. *et al.* Cyclic AMP Produced inside Mitochondria Regulates Oxidative Phosphorylation. *Cell Metab* **9**, 265–276 (2009).
157. Solaini, G., Baracca, A., Lenaz, G. & Sgarbi, G. Hypoxia and mitochondrial oxidative metabolism. *Biochimica et Biophysica Acta (BBA) - Bioenergetics* **1797**, 1171–1177 (2010).
158. Cartron, P. F., Oliver, L., Mayat, E., Meflah, K. & Vallette, F. M. Impact of pH on Bax alpha conformation, oligomerisation and mitochondrial integration. *FEBS Letters* **578**, 41–46 (2004).
159. Green, D. R. & Reed, J. C. Mitochondria and apoptosis. *Science* **281**, 1309–1312 (1998).
160. Li, A., Xue, Y., Jin, C., Wang, M. & Yao, X. Prediction of Nepsilon-acetylation on internal lysines implemented in Bayesian Discriminant Method. *Biochem Biophys Res Commun* **350**, 818–824 (2006).